

Differential Smoothing Mitigates Sharpening and Improves LLM Reasoning

Jingchu Gai^{1*} Guanning Zeng^{2*} Huaqing Zhang^{2*} Aditi Raghunathan¹

¹Carnegie Mellon University, ²Tsinghua University

✉ jgai@cs.cmu.edu, zgn21@mails.tsinghua.edu.cn, zhanghq22@mails.tsinghua.edu.cn, raditi@cmu.edu

Abstract

It is widely recognized that reinforcement learning (RL) fine-tuning of large language models often leads to *diversity collapse*, where outputs lack variety. Prior work has proposed a range of heuristics to counteract this effect, but these methods are ad hoc: they frequently trade off correctness for diversity, their effectiveness varies across tasks, and in some cases they even contradict one another. In this work, we place these observations on a rigorous foundation. We first provide a formal proof of why RL fine-tuning exhibits diversity collapse via a selection and reinforcement bias. Next, we make a key observation that any reward modification to address diversity collapse only needs to be applied on the correct trajectories. Building directly on this analysis, we introduce a principled method—*differential smoothing*—that provably improves both correctness and diversity, outperforming vanilla RL as well as widely used entropy-based heuristics. Our theory precisely characterizes when existing heuristics help and why they fail, while showing that differential smoothing is universally superior. Extensive experiments with models from 1B to 7B parameters, across domains including CountDown and real-world mathematical reasoning, demonstrate consistent gains. Differential smoothing improves both Pass@1 and Pass@k, with up to 6.7% improvements on AIME24 dataset.

1 Introduction

Reinforcement learning (RL) has become a powerful technique for fine-tuning Large Language Models (LLMs), enhancing capabilities ranging from complex reasoning (Guo et al., 2025; Yu et al., 2025; Shao et al., 2024) to human preference alignment (Ouyang et al., 2022; Bai et al., 2022a). However, this process is often plagued by a significant side effect: a collapse in generation diversity (Song et al., 2024; Dang et al., 2025; Yue et al., 2025; Zhao et al., 2025; He et al., 2025a). This degradation is empirically observed in metrics like Pass@K; RL-tuned models often show diminishing improvements for larger values of K and can even underperform the original base model (He et al., 2025a; Cobbe et al., 2021; Chow et al., 2024; Chen et al., 2025b).

However, mitigating this diversity collapse is non-trivial and presents several challenges. Simple heuristics such as early stopping or high-temperature decoding may boost diversity and achieve higher Pass@K, but they frequently hurt Pass@1 performance. This points to an inherent tension between increasing diversity and preserving accuracy. Second, most existing methods lack robustness across settings. A striking example is entropy control, where some works recommend maximizing entropy to improve both Pass@1 and Pass@K, while others report that minimizing entropy can yield the same outcome. Our experiments confirm that prior techniques designed to enhance diversity fail to succeed broadly and often succeed only on the tasks for which they were originally developed.

*Equal contribution

Motivated by these limitations, our work has two primary goals: (1) to provide clarity on the seemingly contradictory effects of previous methods, and (2) to develop a principled method that robustly improves both correctness (Pass@1) and diversity (Pass@K) across a range of benchmarks.

Our analysis from first principles shows that RL fine-tuning introduces two biases, **selection bias** and **reinforcement bias**, which jointly cause diversity collapse within the correct trajectories. Selection bias arises because correct trajectories with high probability under the pre-trained model are more likely to be reinforced (Theorem B.2). Reinforcement bias then arises because these same trajectories receive disproportionately larger updates (Theorem B.3).

Leveraging the insights from our theoretical analysis, we propose a *simple but novel twist* to vanilla RL. The core of our method is that while we need to change the reward function on correct trajectories to prevent the diversity collapse, the incorrect trajectories can continue to use the original reward or even a modification that encourages “sharpening”. This differentiated reward mechanism that applies distinct pressures to correct and incorrect trajectories can provably mitigate the tradeoff between correctness and diversity that plagues other heuristics.

We propose the **differential smoothing** approach. For correct trajectories, our reward mitigates the diversity collapse by subtracting a term proportional to their log-probability. On incorrect trajectories, our reward modification focuses on correctness, by adding the log-probability of the incorrect trace. We present our proposed DS-GRPO algorithm in Section 4.2.

We validate our differential smoothing approach both theoretically and empirically. Our theoretical analysis (Section 3) formally proves that the reward modification for correct trajectories directly optimizes for diversity, while the adjustment for incorrect ones enhances correctness without compromising diversity.

We evaluate DS-GRPO on five different models ranging from 1.5B-8B, and across a range of real-world settings, from simpler tasks such as Countdown to more challenging benchmarks in mathematical reasoning tasks. We consistently observe that DS-GRPO improves both Pass@1 and Pass@K relative to the vanilla baseline; on the Mistral-8B model, DS-GRPO outperforms the baseline by up to 6.7%. We further compare against prior heuristics, including entropy regularization and recent diversity-prompting techniques (He et al., 2025a; Chen et al., 2025c; Walder & Karkhanis, 2025a). While these baselines yield improvements only in certain settings, DS-GRPO delivers robust gains across *all* datasets and models tested. Thus, DS-GRPO represents a principled approach that not only improves upon vanilla RL but also provides consistently stronger results than existing heuristics.

Finally, our analysis clarifies the contradictory effects of global entropy regularization in prior work. Increasing entropy across all trajectories improves diversity but reduces correctness, which can help on tasks with many valid solutions. Conversely, decreasing entropy improves correctness at the cost of diversity, which suits tasks with few valid solutions. Our experiments confirm this principle, and we further show that *differential entropy control*, increasing entropy on correct trajectories while decreasing it on incorrect ones—achieves the best of both, paralleling the effect of differential smoothing.

Summary of Our Main Contribution

1. We analyze diversity collapse from first principles in a formal setting.
2. Based on our diagnosis, we propose a novel differential smoothing algorithm that empirically improves both Pass@1 and Pass@K and outperforms previous methods *robustly* in various real-world settings.
3. We formally prove that our proposed differential smoothing approach improves diversity and correctness over the vanilla approach and the popular entropy maximization heuristic.
4. The analysis in this work also has broader implications of clarifying when and why existing heuristics work and guide the principled modifications of such heuristics.

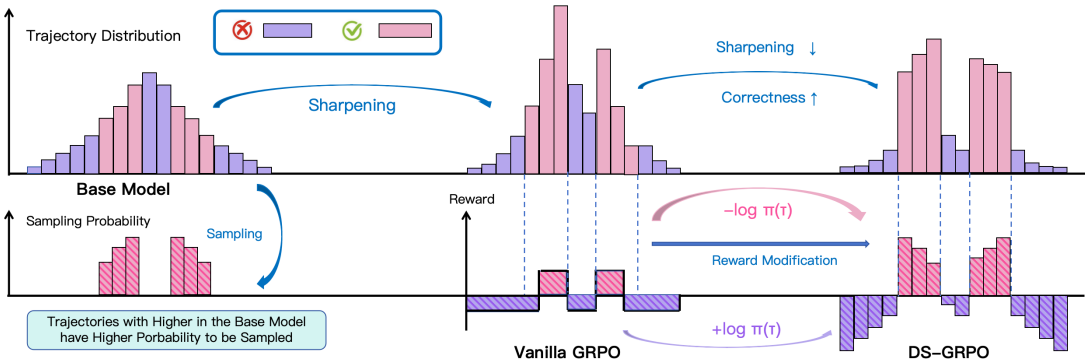


Figure 1: An illustration of the sharpening effect in vanilla RL and the mitigation mechanism of DS-GRPO

2 Related Work

Mitigating Diversity Collapse in RL for Reasoning. Repeated sampling has gained recent attention for significantly improving LLM performance (Sessa et al., 2024; Chow et al., 2024; Wang et al., 2024; Brown et al., 2024; Roziere et al., 2023). However, reinforcement learning fine-tuning is known to cause “diversity collapse”—where the policy sharpens around a few solutions (Dang et al., 2025; Yue et al., 2025)—which directly impairs Pass@K performance (Chen et al., 2025b). Although prior work has empirically documented this effect (Wu et al., 2025), we are the first to rigorously explain its underlying cause in a simple formal setting.

Existing methods to mitigate this issue, such as optimizing for Pass@K (Tang et al., 2025; Walder & Karkhanis, 2025a) or encouraging low-probability solutions (He et al., 2025a; Song et al., 2025), often force a trade-off: they improve diversity (Pass@K) at the expense of correctness (Pass@1) and suffer from widely inconsistent performance. In contrast, our analysis yields a method that fundamentally overcomes this trade-off. To achieve this, we propose a differential modification of the reward function, applying distinct reward structures to correct and incorrect trajectories.

While He et al. (2025a) also employ a differential reward scheme, their method achieves only limited success, performing well on specific tasks but failing on others, such as mathematical reasoning. Our method, however, consistently outperforms their approach across all evaluated tasks. We further provide rigorous theoretical and empirical evidence for the necessity of this differential reward structure.

Controlling Distribution Entropy in RLVR. A common strategy for mitigating diversity collapse and encouraging exploration is to increase policy entropy. However, the precise role and optimal application of entropy regularization remain highly debated. Some studies advocate for entropy maximization to promote exploration and diversity (Yu et al., 2025; He et al., 2025b; Liu et al., 2025). Conversely, other work reports that entropy minimization can improve correctness (Agarwal et al., 2025; Gao et al., 2025). These contradictory findings have created significant uncertainty about the optimal strategy. Our work addresses this ambiguity by interpreting our method as a novel form of conditional entropy control that outperforms these global, uniform strategies. Our analysis clarifies the seemingly disparate effects of entropy manipulation and provides a new principle for its effective regulation.

3 A theoretical perspective on the diversity collapse in RL

In this section, we theoretically analyze the **diversity collapse** phenomenon that arises during the RL fine-tuning of LLMs where the fine-tuned model converges to a limited set of solutions for a given problem, neglecting other valid alternatives. (He et al., 2025a; Song et al., 2025). This diversity collapse leads to a measurable degradation in metrics such as Pass@K as RL progresses, and potentially stifles the model’s creative problem-solving capabilities.

Our analysis proceeds as follows: We first introduce our theoretical abstraction of the RL fine-tuning process (Sec 3.1). We then identify and analyze two primary factors that drive diversity collapse (Sec 3.2). Finally, based on these insights, we derive a principled reward function designed to mitigate this collapse and actively promote solution diversity (Sec 3.2 and Sec 3.4).

3.1 Setup

Preliminaries. We model language generation as a token-level Markov Decision Process (MDP). The environment is defined by a state space \mathcal{S} , a token vocabulary (action space) \mathcal{A} , and a maximum length H . An episode begins with an input prompt $\mathbf{x} \in \mathcal{X}$, which defines the initial state $s_1 = (\mathbf{x})$. At each step h , the state $s_h = (\mathbf{x}, a_1, \dots, a_{h-1}) \in \mathcal{S}_h$ captures the prompt and previously generated tokens. The agent's policy $\pi_h(\cdot|s_h) : \mathcal{S}_h \rightarrow \Delta(\mathcal{A})$ provides a distribution over the next token. State transitions are deterministic: selecting action $a_h \in \mathcal{A}$ in state s_h leads to $s_{h+1} = (\mathbf{x}, a_1, \dots, a_h)$.

A complete trajectory is $\tau = (\mathbf{x}, a_1, \dots, a_H)$, which receives a terminal reward $r(\tau)$. Let \mathcal{C} denote the set of all correct (successful) trajectories. We assume a binary reward function $r(\tau) = \mathbf{1}[\tau \in \mathcal{C}]$. We use an estimated reward function \hat{r} , which is constructed as follows: Initially, $\hat{r}(\tau) = 0$ for all τ . A dataset of trajectories is sampled from base policy π_{base} . A verifier then identifies the subset of successful trajectories. The estimated rewards for these trajectories are subsequently set to 1.

RL fine-tuning over a base policy. A base model (or a pre-trained model) with corresponding policy π_{base} is fine-tuned to optimize the following objective:

$$\pi_{\text{van}}(\tau) = \arg \max_{\pi} \mathbb{E}_{\tau \sim \pi} \hat{r}(\tau) - \beta \cdot \mathbb{D}_{\text{KL}}(\pi || \pi_{\text{base}}), \quad (1)$$

where the KL-divergence term serves as a regularizer that prevents the updated policy from deviating too much from the base policy π_{base} and β is a hyperparameter that balances the trade-off between maximizing reward and preserving the knowledge of the base model. We denote this by π_{van} to distinguish from proposed improvements in later sections.

3.2 Why does RL collapse diversity?

Ideally, RL fine-tuning should increase the likelihood of all correct trajectories. In practice, however, the process disproportionately reinforces correct trajectories that are already high-probability under the base LLM, a phenomenon we refer to as diversity collapse. As a starting point for mitigation, we first formally analyze *why* there is a diversity collapse in the theoretical setup discussed above.

Analysis of Diversity Collapse in Reinforcement Learning

Proposition 3.1 (Selection bias). *The probability that a correct trajectory's likelihood increases is monotonically related to its initial probability under the base model. Formally, for any two correct trajectories τ_1, τ_2 and $\beta > 0$, we have*

$$\pi_{\text{base}}(\tau_1) \geq \pi_{\text{base}}(\tau_2) \implies \mathbb{P}(\pi_{\text{van}}(\tau_1) > \pi_{\text{base}}(\tau_1)) \geq \mathbb{P}(\pi_{\text{van}}(\tau_2) > \pi_{\text{base}}(\tau_2)).$$

Proposition 3.2 (Reinforcement bias). *The magnitude of probability gain for a given correct trajectory is directly proportional to its probability under the base policy. Formally, if the reward update mechanism has access to the complete set of correct trajectories ($\hat{r}(\tau) = 1$ for all correct trajectories), then for any correct trajectory τ and $\beta > 0$, we have*

$$\pi_{\text{van}}(\tau) - \pi_{\text{base}}(\tau) \propto \pi_{\text{base}}(\tau).$$

Proposition 3.1 reveals a *selection bias*: among correct trajectories, those with higher base probabilities are more likely to be reinforced. In addition, Proposition 3.2 shows that there is a *reinforcement bias*: these same high-probability correct trajectories further receive disproportionately larger boosts, further amplifying the model's existing preferences and sharpening the distribution. The proofs for Proposition 3.2 and Proposition 3.1 are provided in Appendix B.1. These results are derived by directly calculating the expression for the fine-tuned policy and analyzing its resulting probability distribution across trajectories. Crucially, the analysis of reinforcement and selection biases pertains specifically to correct trajectories. Conversely, incorrect trajectories exhibit an inverse dynamic: high-probability errors are subject to stronger penalization. Consequently, the probability distribution over incorrect trajectories is flattened rather than sharpened.

3.3 The correctness-diversity tradeoff

A reward function to mitigate diversity collapse. To counter diversity collapse, we modify the reward function to discourage the reinforcement of high-probability trajectories. Since Lemma B.1 implies that $\pi^*(\tau) \propto \exp(\hat{r}(\tau)/\beta)$, we define the modified reward

$$\tilde{r}(\tau) = \hat{r}(\tau) - \underbrace{\gamma_{\text{ent}} \log \pi_{\text{base}}(\tau)}_{\text{entropy bonus}},$$

where $\gamma_{\text{ent}} > 0$ controls the strength of regularization. The additional entropy bonus encourages the policy to assign more weight to trajectories that were less likely under the base policy countering the selection and reinforcement biases.

While such a change is natural, and has been previously proposed, we see that the gains of an entropy bonus are not universal. In Section 4.8 (Fig 4), we test out the entropy bonus objective and find that entropy bonus improves performance on Countdown but hurts performance (and underperforms standard GRPO) on MATH500.

Conversely, other works advocate for an *entropy penalty* i.e. adding rather than subtracting $\gamma_{\text{ent}} \log \pi_{\text{base}}(\tau)$ rather than an entropy bonus to improve performance (Gao et al., 2025; Agarwal et al., 2025). We see that entropy penalty in fact improves performance on MATH500, while underperforming on Countdown.

This apparent contradictory benefits of both entropy bonus and entropy penalty suggests the optimal strategy is task-dependent. Intuitively, entropy bonus improves diversity but at the cost of correctness. Such a tradeoff has also been reported with other methods such as increasing temperature (Dang et al., 2025). On the other hand, entropy penalty does the reverse and improves correctness but at the cost of diversity. For tasks with high inherent diversity in correct solutions, the gain in diversity offers a significant benefit and an entropy bonus overall works out to be beneficial; for tasks with low solution diversity, the increase in diversity does not offer a benefit that outweighs a potential decrease in correctness, and an entropy penalty ends up being beneficial.

We can observe this more precisely by defining a *Solution Multiplicity* metric, defined as the average number of unique correct solutions per problem:

$$\text{Solution Multiplicity}(\mathcal{X}) = \frac{1}{|\mathcal{X}|} \sum_{x \in \mathcal{X}} A(x), \quad (2)$$

where $A(x)$ is the number of correct solutions for problem x .

We experimentally test the performance of entropy bonus/penalty on a few other datasets and find that entropy bonus is more effective when Solution Multiplicity is high, whereas an entropy penalty performs better when it is low (Section 4.8).

Overall, entropy bonus addresses diversity collapse but at the cost of correctness. Furthermore, both entropy maximization and minimization have been proposed as valid modifications, but neither is universally optimal across all tasks.

3.4 A differential approach to mitigating the tradeoff

The natural mitigation of diversity collapse—entropy bonus—is not the perfect solution because it decreases correctness.

Is this tradeoff inherent, or is there a way to simultaneously improve both the correctness and diversity?

We make a key observation: **we only care about diversity over correct (high reward) trajectories**. Also, reinforcement and selection biases pertains specifically to correct trajectories. Hence, one must redefine the desired diversity metric to focus exclusively on correct trajectories.

We formalize our definition in the simple theoretical framework described previously in Section 3.1. We then describe a new differential reward modification that assigns different entropy terms to the positive and negative trajectories. Finally, we theoretically show that our proposed differential loss mitigates the tradeoff between diversity (over high-reward trajectories) and correctness.

Definition 3.3 (Correctness and Correct-Solution Diversity). *For any policy π , we define its correctness as $C(\pi) = \sum_{\tau \in \mathcal{C}} \pi(\tau)$. We use the normalized variance on correct trajectories to measure diversity over correct solutions. Namely, we define $\sigma(\pi) = [\sum_{\tau \in \mathcal{C}} \pi(\tau)^2 - C(\pi)^2]/C(\pi)^2$.*

A small normalized variance indicates that the probability distribution is more uniform (i.e., less "sharp"). In such a distribution, the probability mass is not concentrated on a few high-probability trajectories but is spread more evenly across a wider set of solutions. This directly translates to higher diversity, as a greater variety of trajectories are likely to be sampled. Therefore, a policy with lower normalized variance exhibits higher diversity. Based on this insight, we consider the following differential reward modification:

$$r_{DS}(\tau) = \begin{cases} \hat{r}(\tau) - \gamma_{DS} \cdot \log(\pi_{base}(\tau)) & \text{if } \hat{r}(\tau) > 0 \quad (\text{correct trajectories}) \\ \hat{r}(\tau) & \text{if } \hat{r}(\tau) \leq 0 \quad (\text{incorrect trajectories}). \end{cases} \quad (3)$$

We then proceed to compare π_{DS} that maximizes the reward above, and π_{ent} that maximizes the standard entropy bonus modification to improve diversity.

$$\begin{aligned} \pi_{ent} &= \arg \max_{\pi} \mathbb{E}_{\tau \sim \pi} [\hat{r}(\tau) - \gamma_{ent} \cdot \log(\pi_{base}(\tau))] - \beta_{ent} \cdot \mathbb{D}_{KL}(\pi || \pi_{base}), \\ \pi_{DS} &= \arg \max_{\pi} \mathbb{E}_{\tau \sim \pi} [r_{DS}(\tau)] - \beta_{DS} \cdot \mathbb{D}_{KL}(\pi || \pi_{base}). \end{aligned}$$

Here, β_{ent} and β_{DS} denote the KL coefficients for the two RL algorithms we are comparing, which use different reward modifications. With the definitions above, we aim to show that our differential reward modification performs better in both correctness and diversity. To this end, we present the following theoretical result:

Theoretical Benefit of Differential Reward Modification

Theorem 3.4. *Assume the model have correct estimation for the reward of all trajectories. For any parameters $\gamma_{ent} \geq 0$ and $\beta_{ent} > 0$ used in Eq. 1 (for π_{ent}) that satisfy a proximity constraint $K_{\rho}(\pi_{ent}, \pi_{base}) \leq \kappa$, there exist parameters $\gamma_{DS} \geq 0$ and $\beta_{DS} > 0$ for π_{DS} such that it also satisfies $K_{\rho}(\pi_{DS}, \pi_{base}) \leq \kappa$, and the following inequalities hold:*

$$C(\pi_{DS}) \geq C(\pi_{ent}) \quad \text{and} \quad \sigma(\pi_{DS}) \geq \sigma(\pi_{ent}).$$

This result holds for $K_{\rho}(\pi, \pi_{base}) \in \{\mathbb{D}_{KL}(\pi || \pi_{base}), \mathbb{D}_{KL}(\pi_{base} || \pi), \mathbb{D}_{\chi^2}(\pi || \pi_{base}), \mathbb{D}_{\chi^2}(\pi_{base} || \pi)\}$.

The KL-divergence constraint ($K_{\rho}(\cdot, \pi_{base}) \leq \kappa$) is a practical necessity and a standard assumption in prior work (Setlur et al., 2025). It prevents the fine-tuned policy from deviating excessively from the base model, thereby retaining pre-trained knowledge and avoiding catastrophic forgetting. Thus, Theorem 3.4 demonstrates that differential reward modification (for π_{DS}) achieves superior correctness (C) and diversity (σ) while adhering to the same proximity constraints as the global penalty method (for π_{ent}).

3.5 Differential Smoothing with Entropy Bonus and Entropy Penalty

We proved that increasing entropy on correct trajectories alone can mitigate the tradeoff with correctness. Additionally, our analysis indicates that reducing the entropy (diversity) of incorrect trajectories enhances model correctness without detriment to the diversity of correct generations. With this perspective, let's revisit entropy penalty which we saw improves performance on some tasks with low solution diversity such as MATH500 but underperformed on tasks with high solution diversity such Countdown. Interestingly, theorem 3.4 interestingly holds even if we apply an entropy penalty exclusively on negative trajectories. In other words, an entropy penalty on negative trajectories does not impact the policy's diversity over correct responses and hence such a modification could prevent

Motivated by this finding, as well as the empirical observation that entropy penalties can improve correctness (Gao et al., 2025; Agarwal et al., 2025), we propose our final method. We term this approach Differential Smoothing (DS), which applies an entropy bonus exclusively to positive samples and an entropy penalty

exclusively to negative samples:

$$r_{\text{DS}}(\tau) = \begin{cases} \hat{r}(\tau) - \gamma_p \cdot \log(\pi_{\text{base}}(\tau)) & \text{if } \hat{r}(\tau) > 0 \quad (\text{correct trajectories}) \\ \hat{r}(\tau) + \gamma_n \cdot \log(\pi_{\text{base}}(\tau)) & \text{if } \hat{r}(\tau) \leq 0 \quad (\text{incorrect trajectories}), \end{cases} \quad (4)$$

where $\gamma_p, \gamma_n \geq 0$ are hyperparameters. This formulation generalizes the reward modification strategy in (3). In the following sections, we first detail the implementation of differential smoothing in GRPO. We will then demonstrate empirically that differential smoothing achieves a significant advantage: it simultaneously increases both correctness (Pass@1) and diversity (Pass@K) across different tasks, outperforming other methods that aim to improve diversity.

4 Empirical evaluation of differential smoothing GRPO

In this section, we empirically evaluate the effectiveness of our proposed reward modification (Eq.3) in LLM reinforcement finetuning.

We first recap the popular GRPO algorithm for LLM fine-tuning with RL and present our adaptation, DS-GRPO that incorporates the differential reward described in Section 3.5. We then compare DS-GRPO with GRPO on Countdown and mathematical reasoning. We further compare our proposed method with other methods aimed at improving diversity, including entropy-based approaches and other recently proposed techniques. Our key finding is that DS-GRPO consistently outperforms both GRPO and prior approaches on all tasks. In contrast, previous methods only outperform baselines on a subset of tasks because they fail to resolve the inherent tradeoff between correctness and diversity. We further analyze entropy-based approaches (both entropy bonus and entropy penalty) and show why their gains are uneven and fundamentally limited. In contrast, our differential reward formulation offers a principled way to enhance diversity over correct trajectories, leading to consistent improvements across the board.

4.1 Preliminaries: Group Relative Policy Optimization

We adopt *Group Relative Policy Optimization* (GRPO) (Shao et al., 2024) as our training backbone. For each input x sampled from the training set, the policy decodes a group of G completions $\{y_i\}_{i=1}^G \sim \pi_{\theta_{\text{old}}}(\cdot | x)$, where $\pi_{\theta_{\text{old}}}$ denotes the behavior policy used to collect the batch (the policy parameters at the previous update). Let $r_i = r(y_i)$ be the scalar reward of completion y_i , and denote by $\mu(\{r_j\}_{j=1}^G)$ and $\sigma(\{r_j\}_{j=1}^G)$ the mean and standard deviation of $\{r_j\}_{j=1}^G$, respectively. GRPO replaces the learned critic with a *group baseline* and uses the group-standardized advantage

$$A_i = \frac{r_i - \mu(\{r_j\}_{j=1}^G)}{\sigma(\{r_j\}_{j=1}^G)}. \quad (5)$$

GRPO adopts a clipped objective with a forward KL regularizer to the fixed *base policy* π^b :

$$\mathcal{J}_{\text{GRPO}}(\theta) = \mathbb{E}_x \mathbb{E}_{\{y_i\}_{i=1}^G \sim \pi_{\theta_{\text{old}}}(\cdot | x)} \left[\frac{1}{G} \sum_{i=1}^G \frac{1}{|y_i|} \sum_{t=1}^{|y_i|} \min(\rho_{i,t}(\theta) A_i, \text{clip}(\rho_{i,t}(\theta), 1 - \epsilon, 1 + \epsilon) A_i) - \beta_{\text{KL}} \mathbb{D}_{\text{KL}}(\pi_{\theta} \| \pi^b) \right],$$

where $\rho_{i,t}(\theta) = \frac{\pi_{\theta}(y_{i,t} | x, y_{i,<t})}{\pi_{\theta_{\text{old}}}(y_{i,t} | x, y_{i,<t})}$ is the importance ratio.

4.2 Reward Modification for Mitigating Diversity Collapse

To operationalize the theoretical principles from Section 3.4 within the GRPO framework, we propose *Differential Smoothing GRPO* (DS-GRPO), a novel algorithm that reshapes the advantage function A_i (Equation (6)). This reshaping directly implements our theoretical reward modification for a detailed discussion). Specifically, for successful completions (where $r_i = 1$), we subtract the term $\gamma_p \log \pi_{\theta_{\text{old}}}(y_i | x)$ from the advantage; conversely, for unsuccessful completions, we add the term $\gamma_n \log \pi_{\theta_{\text{old}}}(y_i | x)$.

Differential Smoothing GRPO (DS-GRPO)

$$A_i^{\text{DS}} = A_i + \begin{cases} -\gamma_p \log \pi_{\theta_{\text{old}}}(y_i | x), & \text{if } r_i = 1, \\ +\gamma_n \log \pi_{\theta_{\text{old}}}(y_i | x), & \text{otherwise,} \end{cases} \quad (6)$$

We plug the modified advantages A_i^{DS} into the GRPO objective:

$$\begin{aligned} \mathcal{J}_{\text{DS}}(\theta) = & \mathbb{E}_x \mathbb{E}_{\{y_i\}_{i=1}^G \sim \pi_{\theta_{\text{old}}}(\cdot | q)} \\ & \left[\frac{1}{G} \sum_{i=1}^G \frac{1}{|y_i|} \sum_{t=1}^{|y_i|} \min(\rho_{i,t}(\theta) A_i^{\text{DS}}, \text{clip}(\rho_{i,t}(\theta), 1 - \epsilon, 1 + \epsilon) A_i^{\text{DS}}) - \beta_{\text{KL}} \mathbb{D}_{\text{KL}}(\pi_{\theta} \| \pi^b) \right]. \end{aligned}$$

In our theoretical framework, we employ π_{base} as the bonus and penalty terms within the modified reward function. Notably, our analysis remains valid even if π_{base} is substituted with π . However, for practical implementation, we empirically select $\pi_{\theta_{\text{old}}}$ due to its superior stability. A detailed justification linking the theory to this practical choice is provided in Appendix B.3. We evaluate DS-GRPO on the Countdown and MATH reasoning benchmarks across a range of models. As demonstrated in the subsequent sections, our method consistently improves both correctness (Pass@1) and diversity (Pass@K), outperforming existing diversity-promoting approaches on all evaluation metrics.

4.3 Experimental Setup

We detail our experimental setup below, covering task specifications, model architectures, and hyperparameter configurations.

Countdown. We evaluate the performance of DS-GRPO on the arithmetic reasoning task *Countdown*, where 3 to 4 integers in [1, 99] are provided and the goal is to produce an equation that equals a target number using all given integers exactly once. Following Pan et al. (2025), we use the Qwen2.5-3B-Instruct (Qwen Team, 2024) as the backbone model. For DS-GRPO, we set $\gamma_p = 0.03$, $\gamma_n = 0.01$. More experiment details are given in Appendix C.1.

Math Reasoning. We further explore DS-GRPO on the task of math reasoning. We choose three models with varied sizes and response lengths, Qwen2.5-Math-1.5B (Qwen Team, 2024), Qwen3-1.7B (Qwen Team, 2025), Qwen2.5-Math-7B (Qwen Team, 2024) and Ministrail-8B-Instruct (Jiang et al., 2024). Our training dataset includes 14053 english-written questions from DAPO17k (Yu et al., 2025) dataset and 12000 questions of the MATH12k dataset (Hendrycks et al., 2021). For each model, we train with a batch size of 32 until the training reward saturates, then evaluate on five commonly used benchmarks of math reasoning: MATH500 (Hendrycks et al., 2021), OlympiadBench (He et al., 2024), AMC23 (math ai, 2025), AIME24 (H4, 2025) and AIME25 (OpenCompass, 2025), with a temperature of 0.7. Following DAPO (Yu et al., 2025), we lift the high clip ratio to 0.25 with the low clip ratio remained 0.20, and adopt their length-dependent loss aggregation method. Experimental details are in App.C.3.

4.4 Comparison of DS-GRPO with Vanilla GRPO

As shown in Figure 2, DS-GRPO demonstrates remarkable robustness. It consistently enhances Pass@K (for all K) by $\approx 4\%$ compared to vanilla GRPO. Crucially, these performance gains are accompanied by a $4\times$ inference speedup. (See Appendix D for additional results).

Figure 3 extends our evaluation to three base models and five mathematical reasoning benchmarks. Our strategy yields substantial improvements, with Pass@1 gains of 0.2%–2.9% and Pass@64 gains of 0.5%–6.7% (detailed in Appendix E.1). This demonstrates our method’s ability to improve RL reasoning while mitigating diversity collapse. Furthermore, it delivers significant efficiency gains: DS-GRPO matches the Pass@64 of vanilla GRPO using only $k = 16$ samples—yielding a nearly $4\times$ inference speedup—while simultaneously pushing the maximum achievable Pass@K. This uniform uplift underscores our approach’s efficacy in enhancing both exploration and diversity.

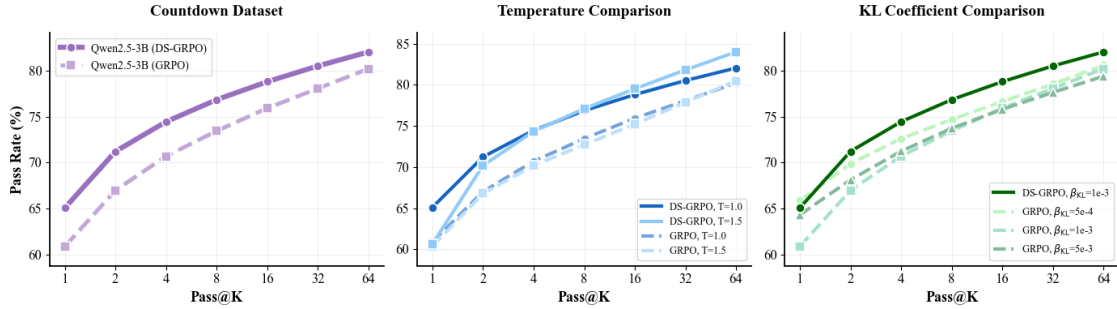


Figure 2: Pass@K performance of DS-GRPO on the Countdown task, compared with GRPO under varying decoding temperatures and KL coefficients.

4.5 Comparison to Base Model

Prior literature (Hochlehnert et al., 2025) indicates that RL fine-tuning can lead to a degradation in Pass@K performance relative to the base model. To demonstrate that our approach mitigates this diversity collapse, we compare the Pass@K metrics of the base model against those of GRPO and DS-GRPO. As shown below, while GRPO exhibits a performance drop compared to the base model, DS-GRPO achieves a consistent improvement. This result confirms that our proposed method effectively alleviates diversity collapse in RL.

Method (Δ)	K=1	K=4	K=16	K=64	K=128	K=512	K=1024	K=2048	K=3072	K=4096	K=6144	K=8192
GRPO - Base	+9.49	+9.57	+7.45	+8.75	+10.25	+9.11	+5.14	+0.71	-1.44	-2.58	-3.68	-3.80
DS-GRPO - Base	+12.73	+11.14	+7.41	+8.27	+9.81	+9.65	+6.81	+3.98	+2.67	+1.91	+1.40	+1.60

4.6 Ablation Experiments on Hyperparameters

To demonstrate the robustness of our method, we further evaluate performance across different hyperparameters, including sampling temperature, the KL coefficient β_{KL} , and the reward modification coefficients γ_p and γ_n .

Temperature and KL Coefficient. We evaluate the stability of DS-GRPO across varying sampling temperatures and KL coefficients (β_{KL}). Our results demonstrate consistent improvements over vanilla GRPO: DS-GRPO enhances Pass@K (for all K) by $\approx 4\%$ across the temperature range and by $\approx 3.2\%$ across different KL coefficients.

Reward Modification Coefficient To isolate the contribution of each component in our reward modification strategy, we conduct an ablation study. We compare the full DS-GRPO algorithm against two specialized variants: *DS-GRPO-Positive*, which only modifies the advantage for correct trajectories, and *DS-GRPO-Negative*, which only modifies the advantage for incorrect trajectories. Their respective advantage modifications are defined as follows:

$$A_i^{DS+} = A_i - \gamma_p \log \pi_{\theta_{old}}(y_i | x), \quad \text{if } r_i = 1, \quad A_i^{DS-} = A_i + \gamma_n \log \pi_{\theta_{old}}(y_i | x), \quad \text{if } r_i \neq 1.$$

The full DS-GRPO algorithm demonstrates superior performance over both of its individual components (DS-GRPO-Positive and DS-GRPO-Negative) for all K . Detailed results and discussion are available in Section E.2. sharpening.

4.7 Comparison with Other Methods for Increasing Diversity

We compare DS-GRPO with prior approaches that encourage diversity in reasoning through reward or advantage shaping, either by optimizing Pass@K rate directly (Tang et al., 2025; Walder & Karkhanis, 2025a; Chen et al., 2025c) or by applying rank-based penalties (He et al., 2025a). For mathematical reasoning experiments, we use the Mistral-8B-Instruct (Jiang et al., 2024) as the base model. For PKPO and GR-PKPO, we use $K = 4$ which performs best in previous work (Chen et al., 2025c); for rank-based penalty, we sweep across various configurations. See more result details in Appendix D.

Pass@K Optimization Methods. Methods that directly optimize the Pass@K metric use it as a reward signal (Tang et al., 2025; Walder & Karkhanis, 2025a; Chen et al., 2025c). However, this approach can

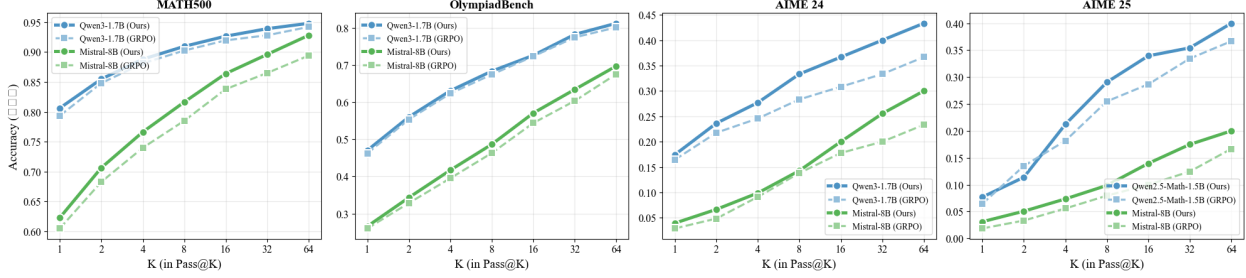


Figure 3: Pass@K performance after reward modification, compared with vanilla GRPO. X-axis denotes K and y-axis denotes pass rates. Trained on DAPO(Yu et al., 2025) and MATH(Hendrycks et al., 2021) Dataset.

assign zero reward to correct solutions, which increases gradient variance and harms training stability. Experimentally, these methods often trade correctness for diversity; for instance, GR-PKPO slightly improves Pass@64 at the cost of Pass@1 and is unstable on the Countdown task (Figure 4, Left). In contrast, DS-GRPO consistently improves Pass@ K across all values of K .

Comparison with Unlikeness Reward Method. Our work is conceptually similar to methods that reward unlikely solutions, such as the one proposed by He et al. (2025a). However, our approach has key advantages. DS-GRPO is derived from a theoretical framework that guarantees its optimality. More critically, it employs a differentiated reward strategy: it modifies rewards for correct trajectories to boost diversity, while a complementary modification for incorrect trajectories improves correctness. In contrast, methods like that of He et al. (2025a) focus solely on diversity, which can harm correctness. Our experimental results (Figure 4) validate this, showing DS-GRPO’s superior performance across all values of K .

Comparison with Other RL Reasoning Methods. We further compare our approach with a recently proposed method that focuses on improving RL reasoning: CISPO (Chen et al., 2025a). Empirical results demonstrate that our method consistently outperforms CISPO across all mathematical reasoning datasets. Detailed comparisons are provided in Appendix E.3.

4.8 Comparing Differential Approach to Entropy Control Method

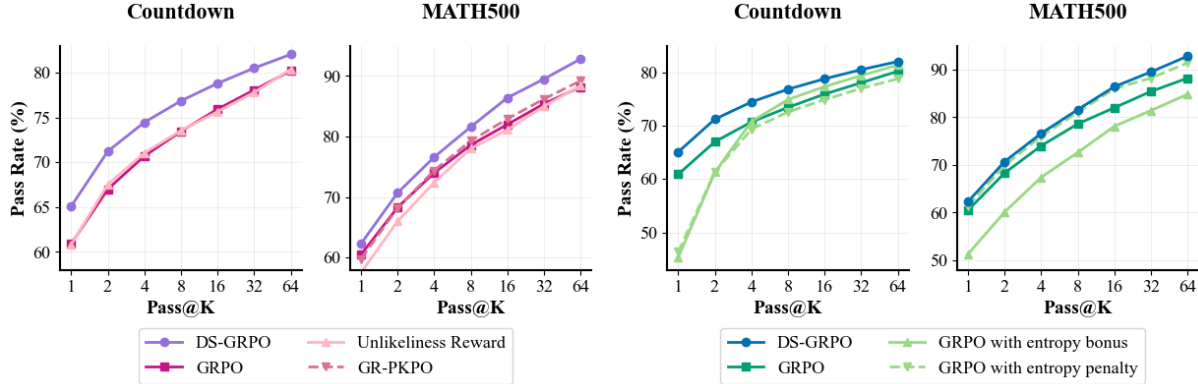


Figure 4: Performance comparisons on MATH500 and Countdown. Left: Comparison among DS-GRPO, GRPO, GR-PKPO (Chen et al., 2025c), and the Unlikeness Reward method (He et al., 2025a). Right: Comparison among DS-GRPO, GRPO, Entropy Regularization, and Entropy Minimization. On the Countdown task, training with GR-PKPO collapses, so results are omitted.

Entropy control is a widely adopted strategy for enhancing the diversity and reasoning capabilities of large language models. In Section 3.4, we have theoretically shown that our differential control approach outperforms both baseline methods and those based on direct entropy maximization. This section presents an empirical comparison of our method against these prior entropy control strategies. We demonstrate that our method achieves superior performance compared to both the vanilla GRPO baseline and GRPO augmented with direct entropy maximization.

4.8.1 DS-GRPO Outperform Entropy Based Method

The role of entropy in RL fine-tuning is complex and subject to ongoing debate. While conventional methods employ entropy regularization to prevent policy collapse (Schulman et al., 2017), recent studies suggest that explicitly *minimizing* entropy can, counter-intuitively, boost performance in certain scenarios (Agarwal et al., 2025; Xingjin Wang, 2025). To position our method within this context, we compare it against two direct entropy control baselines: one that adds an **entropy bonus** to encourage exploration, and one that applies an **entropy penalty** to encourage exploitation. The respective optimization objectives are:

Entropy Based Method

$$\mathcal{J}_{\text{ent}^+} = \mathcal{J}_{\text{GRPO}}(\theta) - \eta_+ \sum_y \pi_\theta(y | x) \log(\pi_\theta(y | x)), \quad \text{Entropy Bonus}$$

$$\mathcal{J}_{\text{ent}^-} = \mathcal{J}_{\text{GRPO}}(\theta) + \eta_- \sum_y \pi_\theta(y | x) \log(\pi_\theta(y | x)), \quad \text{Entropy Penalty}$$

As illustrated in Fig. 4, our method consistently outperforms both the entropy bonus and penalty approaches, regardless of the direction of the regularization. This suggests that a simple, global adjustment to entropy is less effective than our differentiated reward strategy.

4.8.2 Deeper Discussion on Entropy Control

Our experiments (Fig. 4) reveal a critical insight: the effectiveness of global entropy control is highly task-dependent. Specifically, an entropy bonus improves performance over vanilla GRPO on the Countdown task but hinders it on math reasoning benchmarks. Conversely, an entropy penalty benefits math reasoning while degrading performance on Countdown. *Can we explain these differing trends?*

A Principle for Task-Aware Entropy Control. Global entropy bonus does increase diversity but comes at the cost of correctness. This is part of our theoretical argument in Section 3.4. On the other hand, global entropy penalty increases correctness but comes at the cost of diversity. In tasks where diversity is more important, entropy bonus works well but in cases where diversity is less important, entropy penalty works well.

To quantify the importance of solution diversity for a given task, we define Solution Multiplicity in Eq. 2. We measured this metric across four tasks (sampling 200 problems each) and correlated it with the change in Pass@8 performance from adding an entropy bonus. The results are presented in Table 7, with experimental details in Appendix C.4. We conclude that when the number of unique solutions is larger, the benefit of

Task	Knight and Knaves	Math	Countdown-3	Countdown
Solution Multiplicity	1.5	3.7	6.5	15.7
Entropy Effect (for Pass@8)	-9.0%	-6.0%	+1.0%	+3.4%

Table 1: Relationship Between Solution Multiplicity and Entropy Effect

increasing diversity outweighs the potential trade-off in single-solution correctness. Consequently, an entropy bonus is more favorable than an entropy penalty. This leads to our guiding principle for entropy control: for tasks characterized by high Solution Multiplicity, entropy bonus is beneficial but for a task with low Solution Multiplicity, entropy penalty is beneficial.

Differential Control for Correct and Incorrect Trajectories. The underlying mechanism of DS-GRPO is similar to a form of *differentiated entropy control*. An objective function representing this principle can be formulated as:

$$\mathcal{J}_{\text{DS-En}} = \mathcal{J}_{\text{GRPO}} - \eta_p \sum_{y:r(y)>0} \pi_\theta(y | x) \log \pi_\theta(\tau | x) + \eta_n \sum_{y:r(y)\leq 0} \pi_\theta(y | x) \log \pi_\theta(y | x).$$

By selectively increasing entropy only for positive samples, we attain the full diversity benefits of traditional entropy regularization, as we are only concerned with diversity among correct solutions. Concurrently, decreasing entropy for negative samples reinforces correctness. This targeted approach enables simultaneous gains in both correctness (Pass@1) and diversity (Pass@K), offering a more robust and principled method for model fine-tuning across different tasks.

Takeaway: Effect and Principle for Entropy Control

- **Inherent Trade-off:** A global entropy bonus enhances diversity at the cost of correctness, whereas an entropy penalty improves correctness but curtails diversity.
- **Task-Dependent Strategy:** For tasks with high complexity, an entropy bonus is more advantageous. The gains in diversity from exploration outweigh the potential reduction in single-solution accuracy.
- **Superiority of Differentiated Control:** DS-GRPO consistently outperforms both global entropy bonus and penalty strategies. This demonstrates controlling entropy differentially for correct and incorrect trajectories successfully captures the benefits of both approaches—enhancing diversity and reinforcing correctness simultaneously.

5 Conclusion

In this work, we conduct a formal, first-principles analysis of diversity collapse, from which we derive a novel method to enhance policy diversity. We empirically demonstrate that our method outperforms existing approaches and theoretically prove its optimality. Our analysis also clarifies the nuanced, task-dependent role of entropy in fine-tuning, leading to a principled control strategy that simultaneously improves both correctness (Pass@1) and diversity (Pass@K). A formal theoretical analysis of our entropy principle and the nuanced effects of entropy it reveals is left as a promising direction for future research.

6 Acknowledgments

We gratefully acknowledge support from Schmidt Sciences, NSF, Apple, Open Philanthropy, Google. We also thank Gaurav Rohit Ghosal, Manan Agarwal, Sachin Goyal, Kaiyue Wen, Sadhika Malladi, Yuda Song, Akshay Krishnamurthy, Audre He, Xingyu Dang, Chen Wu, Ziqian Zhong, Bingbin Liu for their thoughtful comments and suggestions that helped improve this work.

References

Shivam Agarwal, Zimin Zhang, Lifan Yuan, Jiawei Han, and Hao Peng. The unreasonable effectiveness of entropy minimization in llm reasoning. *arXiv preprint arXiv:2505.15134*, 2025.

Yuntao Bai, Andy Jones, Kamal Ndousse, Amanda Askell, Anna Chen, Nova DasSarma, Dawn Drain, Stanislav Fort, Deep Ganguli, Tom Henighan, et al. Training a helpful and harmless assistant with reinforcement learning from human feedback. *arXiv preprint arXiv:2204.05862*, 2022a.

Yuntao Bai, Saurav Kadavath, Sandipan Kundu, Amanda Askell, Jackson Kernion, Andy Jones, Anna Chen, Anna Goldie, Azalia Mirhoseini, Cameron McKinnon, et al. Constitutional ai: Harmlessness from ai feedback. *arXiv preprint arXiv:2212.08073*, 2022b.

Bradley Brown, Jordan Juravsky, Ryan Ehrlich, Ronald Clark, Quoc V Le, Christopher Ré, and Azalia Mirhoseini. Large language monkeys: Scaling inference compute with repeated sampling. *arXiv preprint arXiv:2407.21787*, 2024.

Aili Chen, Aonian Li, Bangwei Gong, Binyang Jiang, Bo Fei, Bo Yang, Boji Shan, Changqing Yu, Chao Wang, Cheng Zhu, et al. Minimax-m1: Scaling test-time compute efficiently with lightning attention. *arXiv preprint arXiv:2506.13585*, 2025a.

Feng Chen, Allan Raventos, Nan Cheng, Surya Ganguli, and Shaul Druckmann. Rethinking fine-tuning when scaling test-time compute: Limiting confidence improves mathematical reasoning. *arXiv preprint arXiv:2502.07154*, 2025b.

Zhipeng Chen, Xiaobo Qin, Youbin Wu, Yue Ling, Qinghao Ye, Wayne Xin Zhao, and Guang Shi. Pass@ k training for adaptively balancing exploration and exploitation of large reasoning models. *arXiv preprint arXiv:2508.10751*, 2025c.

Daixuan Cheng, Shaohan Huang, Xuekai Zhu, Bo Dai, Wayne Xin Zhao, Zhenliang Zhang, and Furu Wei. Reasoning with exploration: An entropy perspective. *arXiv preprint arXiv:2506.14758*, 2025.

Yinlam Chow, Guy Tennenholz, Izzeddin Gur, Vincent Zhuang, Bo Dai, Sridhar Thiagarajan, Craig Boutilier, Rishabh Agarwal, Aviral Kumar, and Aleksandra Faust. Inference-aware fine-tuning for best-of-n sampling in large language models. *arXiv preprint arXiv:2412.15287*, 2024.

Karl Cobbe, Vineet Kosaraju, Mohammad Bavarian, Mark Chen, Heewoo Jun, Lukasz Kaiser, Matthias Plappert, Jerry Tworek, Jacob Hilton, Reiichiro Nakano, et al. Training verifiers to solve math word problems. *arXiv preprint arXiv:2110.14168*, 2021.

Ganqu Cui, Yuchen Zhang, Jiacheng Chen, Lifan Yuan, Zhi Wang, Yuxin Zuo, Haozhan Li, Yuchen Fan, Huayu Chen, Weize Chen, et al. The entropy mechanism of reinforcement learning for reasoning language models. *arXiv preprint arXiv:2505.22617*, 2025.

Xingyu Dang, Christina Baek, Kaiyue Wen, Zico Kolter, and Aditi Raghunathan. Weight ensembling improves reasoning in language models. *arXiv preprint arXiv:2504.10478*, 2025.

Zitian Gao, Lynx Chen, Haoming Luo, Joey Zhou, and Bryan Dai. One-shot entropy minimization, 2025. URL <https://arxiv.org/abs/2505.20282>.

Daya Guo, Dejian Yang, Haowei Zhang, Junxiao Song, Ruoyu Zhang, Runxin Xu, Qihao Zhu, Shirong Ma, Peiyi Wang, Xiao Bi, et al. Deepseek-r1: Incentivizing reasoning capability in llms via reinforcement learning. *arXiv preprint arXiv:2501.12948*, 2025.

Hugging Face H4. AIME 2024 Dataset (Hugging Face). https://huggingface.co/datasets/HuggingFaceH4/aime_2024, 2025. Accessed: 2025-09-18.

Andre He, Daniel Fried, and Sean Welleck. Rewarding the unlikely: Lifting grp beyond distribution sharpening. *arXiv preprint arXiv:2506.02355*, 2025a.

Chaoqun He, Renjie Luo, Yuzhuo Bai, Shengding Hu, Zhen Leng Thai, Junhao Shen, Jinyi Hu, Xu Han, Yujie Huang, Yuxiang Zhang, Jie Liu, Lei Qi, Zhiyuan Liu, and Maosong Sun. Olympiadbench: A challenging benchmark for promoting agi with olympiad-level bilingual multimodal scientific problems, 2024.

Jujie He, Jiacai Liu, Chris Yuhao Liu, Rui Yan, Chaojie Wang, Peng Cheng, Xiaoyu Zhang, Fuxiang Zhang, Jiacheng Xu, Wei Shen, et al. Skywork open reasoner 1 technical report. *arXiv preprint arXiv:2505.22312*, 2025b.

Dan Hendrycks, Collin Burns, Saurav Kadavath, Akul Arora, Steven Basart, Eric Tang, Dawn Song, and Jacob Steinhardt. Measuring mathematical problem solving with the math dataset. *arXiv preprint arXiv:2103.03874*, 2021.

Andreas Hochlehnert, Hardik Bhatnagar, Vishaal Udandarao, Samuel Albanie, Ameya Prabhu, and Matthias Bethge. A sober look at progress in language model reasoning: Pitfalls and paths to reproducibility. *arXiv preprint arXiv:2504.07086*, 2025.

Edward J Hu, Yelong Shen, Phillip Wallis, Zeyuan Allen-Zhu, Yuanzhi Li, Shean Wang, Lu Wang, Weizhu Chen, et al. Lora: Low-rank adaptation of large language models. *ICLR*, 1(2):3, 2022.

Audrey Huang, Adam Block, Dylan J Foster, Dhruv Rohatgi, Cyril Zhang, Max Simchowitz, Jordan T Ash, and Akshay Krishnamurthy. Self-improvement in language models: The sharpening mechanism. *arXiv preprint arXiv:2412.01951*, 2024.

Jiaxin Huang, Shixiang Shane Gu, Le Hou, Yuexin Wu, Xuezhi Wang, Hongkun Yu, and Jiawei Han. Large language models can self-improve. *arXiv preprint arXiv:2210.11610*, 2022.

Aaron Jaech, Adam Kalai, Adam Lerer, Adam Richardson, Ahmed El-Kishky, Aiden Low, Alec Helyar, Aleksander Madry, Alex Beutel, Alex Carney, et al. Openai o1 system card. *arXiv preprint arXiv:2412.16720*, 2024.

Albert Q. Jiang, Alexandre Sablayrolles, Arthur Mensch, Chris Bamford, Devendra Singh Chaplot, Diego de las Casas, Florian Bressand, Gianna Lengyel, Guillaume Lample, Lucile Saulnier, Lélio Renard Lavaud, Marie-Anne Lachaux, Pierre Stock, Teven Le Scao, Thibaut Lavril, Thomas Wang, Timothée Lacroix, and William El Sayed. Mistral 7b. *arXiv preprint arXiv:2310.06825*, 2024.

Mingjie Liu, Shizhe Diao, Ximing Lu, Jian Hu, Xin Dong, Yejin Choi, Jan Kautz, and Yi Dong. Prorl: Prolonged reinforcement learning expands reasoning boundaries in large language models. *arXiv preprint arXiv:2505.24864*, 2025.

math ai. AMC23 Dataset (Hugging Face). <https://huggingface.co/datasets/math-ai/amc23>, 2025. Accessed: 2025-09-18.

OpenCompass. AIME 2025 Dataset (Hugging Face). <https://huggingface.co/datasets/opencompass/AIME2025>, 2025. Accessed: 2025-09-18.

Long Ouyang, Jeffrey Wu, Xu Jiang, Diogo Almeida, Carroll Wainwright, Pamela Mishkin, Chong Zhang, Sandhini Agarwal, Katarina Slama, Alex Ray, et al. Training language models to follow instructions with human feedback. *Advances in neural information processing systems*, 35:27730–27744, 2022.

Jiayi Pan, Junjie Zhang, Xingyao Wang, Lifan Yuan, Hao Peng, and Alane Suhr. Tinyzero. <https://github.com/Jiayi-Pan/TinyZero>, 2025. Accessed: 2025-01-24.

Jing-Cheng Pang, Pengyuan Wang, Kaiyuan Li, Xiong-Hui Chen, Jiacheng Xu, Zongzhang Zhang, and Yang Yu. Language model self-improvement by reinforcement learning contemplation. *arXiv preprint arXiv:2305.14483*, 2023.

Qwen Team. Qwen2.5: A party of foundation models, September 2024. URL <https://qwenlm.github.io/blog/qwen2.5/>.

Qwen Team. Qwen3 technical report, 2025. URL <https://arxiv.org/abs/2505.09388>.

Baptiste Roziere, Jonas Gehring, Fabian Gloeckle, Sten Sootla, Itai Gat, Xiaoqing Ellen Tan, Yossi Adi, Jingyu Liu, Romain Sauvestre, Tal Remez, et al. Code llama: Open foundation models for code. *arXiv preprint arXiv:2308.12950*, 2023.

John Schulman, Filip Wolski, Prafulla Dhariwal, Alec Radford, and Oleg Klimov. Proximal policy optimization algorithms. *arXiv preprint arXiv:1707.06347*, 2017.

Pier Giuseppe Sessa, Robert Dadashi, Léonard Hussenot, Johan Ferret, Nino Vieillard, Alexandre Ramé, Bobak Shariari, Sarah Perrin, Abe Friesen, Geoffrey Cideron, et al. Bond: Aligning llms with best-of-n distillation, 2024. URL <https://arxiv.org/abs/2407.14622>.

Amrith Setlur, Nived Rajaraman, Sergey Levine, and Aviral Kumar. Scaling test-time compute without verification or rl is suboptimal. *arXiv preprint arXiv:2502.12118*, 2025.

Zhihong Shao, Peiyi Wang, Qihao Zhu, Runxin Xu, Junxiao Song, Xiao Bi, Haowei Zhang, Mingchuan Zhang, YK Li, Y Wu, et al. Deepseekmath: Pushing the limits of mathematical reasoning in open language models, 2024. URL <https://arxiv.org/abs/2402.03300>, 2(3):5, 2024.

Yuda Song, Hanlin Zhang, Carson Eisenach, Sham Kakade, Dean Foster, and Udaya Ghai. Mind the gap: Examining the self-improvement capabilities of large language models. *arXiv preprint arXiv:2412.02674*, 2024.

Yuda Song, Julia Kempe, and Remi Munos. Outcome-based exploration for llm reasoning, 2025. URL <https://arxiv.org/abs/2509.06941>.

Zafir Stojanovski, Oliver Stanley, Joe Sharratt, Richard Jones, Abdulhakeem Adefioye, Jean Kaddour, and Andreas Köpf. Reasoning gym: Reasoning environments for reinforcement learning with verifiable rewards. *arXiv preprint arXiv:2505.24760*, 2025.

Yunhao Tang, Kunhao Zheng, Gabriel Synnaeve, and Rémi Munos. Optimizing language models for inference time objectives using reinforcement learning. *arXiv preprint arXiv:2503.19595*, 2025.

Christian Walder and Deep Karkhanis. Pass@ k policy optimization: Solving harder reinforcement learning problems. *arXiv preprint arXiv:2505.15201*, 2025a.

Christian Walder and Deep Karkhanis. Pass@k policy optimization: Solving harder reinforcement learning problems, 2025b. URL <https://arxiv.org/abs/2505.15201>.

Peiyi Wang, Lei Li, Zhihong Shao, Runxin Xu, Damai Dai, Yifei Li, Deli Chen, Yu Wu, and Zhifang Sui. Math-shepherd: Verify and reinforce llms step-by-step without human annotations. In *Proceedings of the 62nd Annual Meeting of the Association for Computational Linguistics (Volume 1: Long Papers)*, pp. 9426–9439, 2024.

Shenzi Wang, Le Yu, Chang Gao, Chujie Zheng, Shixuan Liu, Rui Lu, Kai Dang, Xionghui Chen, Jianxin Yang, Zhenru Zhang, Yuqiong Liu, An Yang, Andrew Zhao, Yang Yue, Shiji Song, Bowen Yu, Gao Huang, and Junyang Lin. Beyond the 80/20 rule: High-entropy minority tokens drive effective reinforcement learning for llm reasoning, 2025. URL <https://arxiv.org/abs/2506.01939>.

Yizhong Wang, Yeganeh Kordi, Swaroop Mishra, Alisa Liu, Noah A Smith, Daniel Khashabi, and Hannaneh Hajishirzi. Self-instruct: Aligning language models with self-generated instructions. *arXiv preprint arXiv:2212.10560*, 2022.

Fang Wu, Weihao Xuan, Ximing Lu, Zaid Harchaoui, and Yejin Choi. The invisible leash: Why rlrv may not escape its origin. *arXiv preprint arXiv:2507.14843*, 2025.

Lu Wang Xingjin Wang, Howe Tissue. Blog of entropy scheduling, 2025. URL <https://howetissue.notion.site>.

Qiyi Yu, Zheng Zhang, Ruofei Zhu, Yufeng Yuan, Xiaochen Zuo, Yu Yue, Weinan Dai, Tiantian Fan, Gaohong Liu, Lingjun Liu, et al. Dapo: An open-source llm reinforcement learning system at scale. *arXiv preprint arXiv:2503.14476*, 2025.

Yang Yue, Zhiqi Chen, Rui Lu, Andrew Zhao, Zhaokai Wang, Shiji Song, and Gao Huang. Does reinforcement learning really incentivize reasoning capacity in llms beyond the base model? *arXiv preprint arXiv:2504.13837*, 2025.

Rosie Zhao, Alexandru Meterez, Sham Kakade, Cengiz Pehlevan, Samy Jelassi, and Eran Malach. Echo chamber: RL post-training amplifies behaviors learned in pretraining. *arXiv preprint arXiv:2504.07912*, 2025.

Xinyu Zhu, Mengzhou Xia, Zhepei Wei, Wei-Lin Chen, Danqi Chen, and Yu Meng. The surprising effectiveness of negative reinforcement in llm reasoning. *arXiv preprint arXiv:2506.01347*, 2025.

Appendix

A Additional Related Work

Mitigating diversity collapse in the RL of reasoning models Reinforcement Learning with Verifiable Rewards (RLVR) has emerged as the dominant paradigm for enhancing LLM reasoning on tasks like mathematics and programming (Guo et al., 2025; Jaech et al., 2024). This process is often framed as "sharpening," where the model learns to place greater probability mass on high-quality sequences, thereby amortizing the high inference-time cost of generation (Huang et al., 2024; 2022; Wang et al., 2022; Bai et al., 2022b; Pang et al., 2023).

However, this self-improvement risks reducing creativity. Recent studies observe that RLVR often induces "diversity collapse," where the generation distribution becomes overly concentrated (Dang et al., 2025; Yue et al., 2025). This collapse manifests empirically: despite higher pass@1 performance, models trained with RLVR (RLVR-trained models) often underperform their base model on pass@k for large k . This degradation limits test-time scaling and raises a fundamental question: does RLVR truly expand a model's reasoning capabilities, or does it merely sharpen the probability mass around solutions already present in the base distribution (Wu et al., 2025; Yue et al., 2025)?

To mitigate the problem of diversity collapse, a variety of approaches have been proposed from different perspectives. From the algorithm side, Yu et al. (2025) clip-higher strategy and the removal of KL divergence penalties in the GRPO of reasoning models, while He et al. (2025b) suggests adaptively using entropy as a form of regularization. Zhu et al. (2025) shows positive samples in RLVR sharpens the distribution around the sampled correct trajectories, whereas penalizing negative samples preserves diversity, motivating a higher weighting of negative samples in the training objective. In terms of reward design, several studies have proposed making rewards explicitly diversity-aware. Walder & Karkhanis (2025a); Chen et al. (2025c) suggest directly using pass@k metric as the reward. He et al. (2025a) introduces rank-based penalties within sampled groups to encourage diverse output, while Cui et al. (2025) incorporate entropy into advantage estimation to promote exploration. Other methods include interpolate the weights of the base model and the fine-tuned model (Dang et al., 2025).

Controlling distribution entropy in RLVR The entropy of the policy distribution is a key internal indicator of a model's exploration capability(Cui et al., 2025; Cheng et al., 2025). Various methods have been proposed to maintain high entropy during training in order to encourage exploration, including clipping higher, adding entropy bonus (Yu et al., 2025; He et al., 2025b), or selectively training on critical high-entropy tokens (Wang et al., 2025). Other studies report that RLVR improves performance at the expense of reduced policy entropy (Cui et al., 2025), and that simply minimizing entropy can effectively improve pass@1 accuracy(Agarwal et al., 2025; Gao et al., 2025). Xingjin Wang (2025) further propose an entropy scheduling approach that maintains high entropy in the early stage to encourage exploration and reduces entropy later to improve final performance. In contrast to prior approaches, we treat correct and incorrect samples separately: bonusing entropy for correct samples and penalizing entropy for incorrect ones. We demonstrate the superiority of this design both theoretically and empirically.

B Proof of Theorems

B.1 Proof of Proposition B.2 and Proposition B.3

Lemma B.1. *The solution to the KL-regularized optimization problem:*

$$\pi_{\beta_{\text{ent}}}^* = \arg \max_{\pi} \{ \mathbb{E}_{\tau \sim \pi} r(\tau) - \beta_{\text{ent}} \cdot \mathbb{D}_{\text{KL}}(\pi || \pi_{\text{base}}) \}$$

has the following closed-form expression for a trajectory τ :

$$\pi_{\beta_{\text{ent}}(\tau)}^* = \frac{\left[\prod_{h=1}^H \pi_{\text{base},h}(a_h | s_h) \right] \exp\left(\frac{1}{\beta_{\text{ent}}} r(\tau)\right)}{\sum_{\tau': s'_1=s} \left[\prod_{h=1}^H \pi_{\text{base},h}(a'_h | s'_h) \right] \exp\left(\frac{1}{\beta_{\text{ent}}} r(\tau')\right)},$$

where the summation in the denominator is over all valid trajectories τ' starting from the initial state s .

Proof. The optimization problem can be written as finding a probability distribution $\pi(\tau)$ over trajectories that solves:

$$\max_{\pi} \sum_{\tau} \pi(\tau) r(\tau) - \beta_{\text{ent}} \sum_{\tau} \pi(\tau) \ln\left(\frac{\pi(\tau)}{\pi_{\text{base}}(\tau)}\right), \quad \text{subject to} \quad \sum_{\tau} \pi(\tau) = 1.$$

We introduce a Lagrange multiplier μ for the probability constraint and form the Lagrangian $\mathcal{L}(\pi, \mu)$:

$$\mathcal{L}(\pi, \mu) = \sum_{\tau} \pi(\tau) r(\tau) - \beta_{\text{ent}} \sum_{\tau} \pi(\tau) [\ln(\pi(\tau)) - \ln(\pi_{\text{base}}(\tau))] - \mu \left(\sum_{\tau} \pi(\tau) - 1 \right).$$

To find the optimal policy, we take the partial derivative of \mathcal{L} with respect to $\pi(\tau)$ and set it to zero:

$$\frac{\partial \mathcal{L}}{\partial \pi(\tau)} = r(\tau) - \beta_{\text{ent}} \left(\ln\left(\frac{\pi(\tau)}{\pi_{\text{base}}(\tau)}\right) + 1 \right) - \mu = 0.$$

Solving for $\pi(\tau)$, we obtain:

$$\begin{aligned} \ln\left(\frac{\pi(\tau)}{\pi_{\text{base}}(\tau)}\right) &= \frac{r(\tau)}{\beta_{\text{ent}}} - 1 - \frac{\mu}{\beta_{\text{ent}}} \\ \Rightarrow \pi(\tau) &= \pi_{\text{base}}(\tau) \exp\left(\frac{r(\tau)}{\beta_{\text{ent}}} - 1 - \frac{\mu}{\beta_{\text{ent}}}\right) = \pi_{\text{base}}(\tau) \exp\left(\frac{r(\tau)}{\beta_{\text{ent}}}\right) \exp\left(-1 - \frac{\mu}{\beta_{\text{ent}}}\right). \end{aligned}$$

The term $\exp(-1 - \mu/\beta_{\text{ent}})$ is a constant determined by the normalization constraint $\sum_{\tau'} \pi(\tau') = 1$. Let the partition function be $\mathcal{Z} = \sum_{\tau'} \pi_{\text{base}}(\tau') \exp\left(\frac{r(\tau')}{\beta_{\text{ent}}}\right)$. The normalization constant must be $1/\mathcal{Z}$, which gives the solution:

$$\pi_{\beta_{\text{ent}}}^*(\tau) = \frac{\pi_{\text{base}}(\tau) \exp\left(\frac{1}{\beta_{\text{ent}}} r(\tau)\right)}{\mathcal{Z}} = \frac{\pi_{\text{base}}(\tau) \exp\left(\frac{1}{\beta_{\text{ent}}} r(\tau)\right)}{\sum_{\tau'} \pi_{\text{base}}(\tau') \exp\left(\frac{1}{\beta_{\text{ent}}} r(\tau')\right)}.$$

By substituting the definitions $\pi_{\text{base}}(\tau) = \prod_{h=1}^H \pi_{\text{base},h}(a_h | s_h)$, we arrive at the expression stated in the lemma. This completes the proof. \square

Proposition B.2 (Selection Bias). *The probability that a correct trajectory's likelihood increases is monotonically related to its initial probability under the base model. Formally, for any two correct trajectories τ_1, τ_2 and $\beta_{\text{ent}} > 0$, we have*

$$\pi_{\text{base}}(\tau_1) \geq \pi_{\text{base}}(\tau_2) \implies \mathbb{P}(\pi_{\text{van}}(\tau_1) > \pi_{\text{base}}(\tau_1)) \geq \mathbb{P}(\pi_{\text{van}}(\tau_2) > \pi_{\text{base}}(\tau_2)).$$

Proposition B.3 (Reinforcement bias). *The magnitude of probability gain for a given trajectory is directly proportional to its probability under the base policy. Formally, if the reward update mechanism has access to the complete set of correct trajectories ($r(\tau) = 1$ for all correct trajectories), then for any trajectory τ and $\beta_{\text{ent}} > 0$, we have*

$$\pi_{\text{van}}(\tau) - \pi_{\text{base}}(\tau) \propto \pi_{\text{base}}(\tau).$$

Proof. **Part 1: Monotonicity of Likelihood Improvement.** Under the specified reward mechanism, a correct trajectory τ receives a positive reward if it is not missed in all N independent samples. This occurs with probability $1 - (1 - \pi_{\text{base}}(\tau))^N$. A positive reward ensures that the likelihood of the trajectory increases after fine-tuning. Thus, the probability of improvement is:

$$\mathbb{P}(\pi_{\text{van}}(\tau) > \pi_{\text{base}}(\tau)) = 1 - (1 - \pi_{\text{base}}(\tau))^N.$$

This function is monotonically increasing with respect to $\pi_{\text{base}}(\tau)$ for $\pi_{\text{base}}(\tau) \in [0, 1]$. Therefore, if $\pi_{\text{base}}(\tau_1) \geq \pi_{\text{base}}(\tau_2)$, the first claim holds.

Part 2: Proportionality of Probability Gain. From the closed-form solution for the optimal policy (as derived in Lemma B.1), we have $\pi_{\beta_{\text{ent}}}^*(\tau) = \pi_{\text{base}}(\tau) \exp(r(\tau)/\beta_{\text{ent}})/\mathcal{Z}$, where \mathcal{Z} is the partition function. The change in probability is:

$$\pi_{\beta_{\text{ent}}}^*(\tau) - \pi_{\text{base}}(\tau) = \frac{\pi_{\text{base}}(\tau) \exp(r(\tau)/\beta_{\text{ent}})}{\mathcal{Z}} - \pi_{\text{base}}(\tau) = \pi_{\text{base}}(\tau) \left[\frac{\exp(r(\tau)/\beta_{\text{ent}}) - \mathcal{Z}}{\mathcal{Z}} \right].$$

The partition function $\mathcal{Z} = \sum_{\tau'} \pi_{\text{base}}(\tau') \exp(r(\tau')/\beta_{\text{ent}})$ is a constant for a given policy π_{base} and reward function r . The term in the brackets is therefore constant for all trajectories τ that share the same reward value (e.g., all correct trajectories). Consequently, the probability gain is directly proportional to the initial probability $\pi_{\text{base}}(\tau)$. \square

B.2 Proof of Theorem 3.4

Lemma B.4. *The solution to the KL-regularized optimization problem with an entropy-based reward modification:*

$$\pi_{\beta_{\text{ent}}, \gamma_{\text{ent}}}^* = \arg \max_{\pi} \{ \mathbb{E}_{\tau \sim \pi} [r(\tau) - \gamma_{\text{ent}} \log(\pi_{\text{base}}(\tau))] - \beta_{\text{ent}} \cdot \mathbb{D}_{\text{KL}}(\pi || \pi_{\text{base}}) \}$$

is given by:

$$\pi_{\beta_{\text{ent}}, \gamma_{\text{ent}}}^*(\tau) = \frac{[\pi_{\text{base}}(\tau)]^{1 - \frac{\gamma_{\text{ent}}}{\beta_{\text{ent}}}} \exp\left(\frac{1}{\beta_{\text{ent}}} r(\tau)\right)}{\sum_{\tau'} [\pi_{\text{base}}(\tau')]^{1 - \frac{\gamma_{\text{ent}}}{\beta_{\text{ent}}}} \exp\left(\frac{1}{\beta_{\text{ent}}} r(\tau')\right)},$$

where the summation in the denominator is over all valid trajectories τ' .

Proof. The objective function can be expanded as:

$$\max_{\pi} \sum_{\tau} \pi(\tau) (r(\tau) - \gamma_{\text{ent}} \log(\pi_{\text{base}}(\tau))) - \beta_{\text{ent}} \sum_{\tau} \pi(\tau) \ln\left(\frac{\pi(\tau)}{\pi_{\text{base}}(\tau)}\right),$$

subject to the constraint $\sum_{\tau} \pi(\tau) = 1$. We form the Lagrangian $\mathcal{L}(\pi, \mu)$:

$$\begin{aligned} & \mathcal{L}(\pi, \mu) \\ &= \sum_{\tau} \pi(\tau) (r(\tau) - \gamma_{\text{ent}} \log(\pi_{\text{base}}(\tau))) - \beta_{\text{ent}} \sum_{\tau} \pi(\tau) (\ln(\pi(\tau)) - \ln(\pi_{\text{base}}(\tau))) - \mu \left(\sum_{\tau} \pi(\tau) - 1 \right). \end{aligned}$$

Setting the partial derivative with respect to $\pi(\tau)$ to zero yields:

$$\frac{\partial \mathcal{L}}{\partial \pi(\tau)} = r(\tau) - \gamma_{\text{ent}} \log(\pi_{\text{base}}(\tau)) - \beta_{\text{ent}} \left(\ln\left(\frac{\pi(\tau)}{\pi_{\text{base}}(\tau)}\right) + 1 \right) - \mu = 0.$$

Solving for $\pi(\tau)$:

$$\begin{aligned}
 \ln \left(\frac{\pi(\tau)}{\pi_{\text{base}}(\tau)} \right) &= \frac{r(\tau)}{\beta_{\text{ent}}} - \frac{\gamma_{\text{ent}}}{\beta_{\text{ent}}} \log(\pi_{\text{base}}(\tau)) - 1 - \frac{\mu}{\beta_{\text{ent}}} \\
 \implies \pi(\tau) &= \pi_{\text{base}}(\tau) \exp \left(\frac{r(\tau)}{\beta_{\text{ent}}} - \frac{\gamma_{\text{ent}}}{\beta_{\text{ent}}} \log(\pi_{\text{base}}(\tau)) - 1 - \frac{\mu}{\beta_{\text{ent}}} \right) \\
 &= \pi_{\text{base}}(\tau) \cdot (\exp(\log(\pi_{\text{base}}(\tau))))^{-\frac{\gamma_{\text{ent}}}{\beta_{\text{ent}}}} \cdot \exp \left(\frac{r(\tau)}{\beta_{\text{ent}}} \right) \cdot \exp \left(-1 - \frac{\mu}{\beta_{\text{ent}}} \right) \\
 &= [\pi_{\text{base}}(\tau)]^{1-\frac{\gamma_{\text{ent}}}{\beta_{\text{ent}}}} \exp \left(\frac{r(\tau)}{\beta_{\text{ent}}} \right) \exp \left(-1 - \frac{\mu}{\beta_{\text{ent}}} \right).
 \end{aligned}$$

The term $\exp(-1 - \mu/\beta_{\text{ent}})$ is a normalization constant. By enforcing the constraint $\sum_{\tau'} \pi(\tau') = 1$, we find that this constant is the reciprocal of the partition function $\mathcal{Z} = \sum_{\tau'} [\pi_{\text{base}}(\tau')]^{1-\frac{\gamma_{\text{ent}}}{\beta_{\text{ent}}}} \exp(r(\tau')/\beta_{\text{ent}})$. This gives the final solution stated in the lemma. \square

Lemma B.5. Consider the reward function $r_{\text{DS}}(\tau)$ which modifies the reward based on trajectory correctness, defined by a set of correct trajectories \mathcal{C} :

$$r_{\text{DS}}(\tau) = \begin{cases} r(\tau) - \gamma_{\text{DS}} \log(\pi_{\text{base}}(\tau)) & \text{if } \tau \in \mathcal{C} \\ r(\tau) & \text{if } \tau \notin \mathcal{C} \end{cases}$$

The solution to the KL-regularized optimization problem $\pi_{\text{DS}} = \arg \max_{\pi} \{ \mathbb{E}_{\tau \sim \pi} [r_{\text{DS}}(\tau)] - \beta_{\text{DS}} \cdot \mathbb{D}_{\text{KL}}(\pi \parallel \pi_{\text{base}}) \}$ is given by:

$$\pi_{\text{DS}}(\tau) = \frac{1}{\mathcal{Z}} \times \begin{cases} [\pi_{\text{base}}(\tau)]^{1-\frac{\gamma_{\text{DS}}}{\beta_{\text{DS}}}} \exp \left(\frac{1}{\beta_{\text{DS}}} r(\tau) \right) & \text{if } \tau \in \mathcal{C} \\ [\pi_{\text{base}}(\tau)] \cdot \exp \left(\frac{1}{\beta_{\text{DS}}} r(\tau) \right) & \text{if } \tau \notin \mathcal{C} \end{cases}$$

where \mathcal{Z} is the partition function ensuring normalization.

Proof. The objective function is maximized subject to $\sum_{\tau} \pi(\tau) = 1$. The Lagrangian is:

$$\begin{aligned}
 \mathcal{L}(\pi, \mu) &= \sum_{\tau \in \mathcal{C}} \pi(\tau) (r(\tau) - \gamma_{\text{DS}} \log(\pi_{\text{base}}(\tau))) + \sum_{\tau \notin \mathcal{C}} \pi(\tau) r(\tau) \\
 &\quad - \beta_{\text{DS}} \sum_{\tau} \pi(\tau) (\ln(\pi(\tau)) - \ln(\pi_{\text{base}}(\tau))) - \mu \left(\sum_{\tau} \pi(\tau) - 1 \right).
 \end{aligned}$$

We take the partial derivative with respect to $\pi(\tau)$ for each case and set it to zero.

For a correct trajectory, $\tau \in \mathcal{C}$:

$$\frac{\partial \mathcal{L}}{\partial \pi(\tau)} = r(\tau) - \gamma_{\text{DS}} \log(\pi_{\text{base}}(\tau)) - \beta_{\text{DS}} \left(\ln \left(\frac{\pi(\tau)}{\pi_{\text{base}}(\tau)} \right) + 1 \right) - \mu = 0.$$

Solving for $\pi(\tau)$ yields: $\pi(\tau) \propto [\pi_{\text{base}}(\tau)]^{1-\frac{\gamma_{\text{DS}}}{\beta_{\text{DS}}}} \exp \left(\frac{r(\tau)}{\beta_{\text{DS}}} \right)$.

For an incorrect trajectory, $\tau \notin \mathcal{C}$:

$$\frac{\partial \mathcal{L}}{\partial \pi(\tau)} = r(\tau) - \beta_{\text{DS}} \cdot \left(\ln \left(\frac{\pi(\tau)}{\pi_{\text{base}}(\tau)} \right) + 1 \right) - \mu = 0.$$

Solving for $\pi(\tau)$ yields: $\pi(\tau) \propto [\pi_{\text{base}}(\tau)] \cdot \exp \left(\frac{r(\tau)}{\beta_{\text{ent}}} \right)$.

Combining these results, the unnormalized solution $\tilde{\pi}(\tau)$ is:

$$\tilde{\pi}(\tau) = \begin{cases} [\pi_{\text{base}}(\tau)]^{1-\frac{\gamma_{\text{DS}}}{\beta_{\text{ent}}}} \exp \left(\frac{1}{\beta_{\text{ent}}} r(\tau) \right) & \text{if } \tau \in \mathcal{C} \\ [\pi_{\text{base}}(\tau)] \cdot \exp \left(\frac{1}{\beta_{\text{ent}}} r(\tau) \right) & \text{if } \tau \notin \mathcal{C} \end{cases}$$

The final solution π_{DS} is obtained by normalizing $\tilde{\pi}(\tau)$ with the partition function $\mathcal{Z} = \sum_{\tau'} \tilde{\pi}(\tau')$, which gives the expression stated in the lemma. \square

Lemma B.6 (Correctness under Reverse KL Constraint). *When $K_\rho(\pi, \pi_{base}) = \mathbb{D}_{KL}(\pi_{base} \parallel \pi)$, for any $\gamma_{ent} \geq 0, \beta_{ent} > 0$ such that $\mathbb{D}_{KL}(\pi_{base} \parallel \pi_{ent}) \leq \kappa$, there exist $\gamma_{DS} \geq 0$ and $\beta_{DS} > 0$ such that $\mathbb{D}_{KL}(\pi_{base} \parallel \pi_{DS}) \leq \kappa$ and $C(\pi_{DS}) \geq C(\pi_{ent})$.*

Proof. To simplify the notation, we define the following sums over trajectory probabilities, where \mathcal{C} is the set of correct trajectories:

$$b_x = \sum_{\tau \in \mathcal{C}} [\pi_{base}(\tau)]^{1-x}, \quad B_x = \sum_{\tau} [\pi_{base}(\tau)]^{1-x}, \quad p_c = \sum_{\tau \in \mathcal{C}} \pi_{base}(\tau).$$

The proof proceeds in three steps: we first find a functional relationship between correctness C and the KL divergence for each policy, and then compare them.

Step 1: Analyze the Entropy-Maximization Policy (π_{ent}). The correctness is the total probability mass on correct trajectories:

$$C(\pi_{ent}) = \frac{\sum_{\tau \in \mathcal{C}} [\pi_{base}(\tau)]^{1-\frac{\gamma_{ent}}{\beta_{ent}}} \exp(1/\beta_{ent})}{\sum_{\tau \in \mathcal{C}} [\pi_{base}(\tau)]^{1-\frac{\gamma_{ent}}{\beta_{ent}}} \exp(1/\beta_{ent}) + \sum_{\tau \notin \mathcal{C}} [\pi_{base}(\tau)]^{1-\frac{\gamma_{ent}}{\beta_{ent}}}} = \frac{b_{\frac{\gamma_{ent}}{\beta_{ent}}} e^{1/\beta_{ent}}}{b_{\frac{\gamma_{ent}}{\beta_{ent}}} e^{1/\beta_{ent}} + (B_{\frac{\gamma_{ent}}{\beta_{ent}}} - b_{\frac{\gamma_{ent}}{\beta_{ent}}})}.$$

Solving for $e^{1/\beta_{ent}}$ gives: $e^{1/\beta_{ent}} = \frac{B_{\frac{\gamma_{ent}}{\beta_{ent}}} - b_{\frac{\gamma_{ent}}{\beta_{ent}}}}{b_{\frac{\gamma_{ent}}{\beta_{ent}}}} \left(\frac{C(\pi_{ent})}{1 - C(\pi_{ent})} \right)$. The reverse KL divergence is $\mathbb{D}_{KL}(\pi_{base} \parallel \pi_{ent}) = \sum_{\tau} \pi_{base}(\tau) \ln(\pi_{base}(\tau) / \pi_{ent}(\tau))$. Substituting the policy definition:

$$\begin{aligned} \mathbb{D}_{KL}(\pi_{base} \parallel \pi_{ent}) &= \frac{\gamma_{ent}}{\beta_{ent}} \sum_{\tau} \pi_{base} \ln \pi_{base} - \frac{1}{\beta_{ent}} \sum_{\tau} \pi_{base} \cdot r(\tau) + \ln \left(b_{\frac{\gamma_{ent}}{\beta_{ent}}} e^{1/\beta_{ent}} + B_{\frac{\gamma_{ent}}{\beta_{ent}}} - b_{\frac{\gamma_{ent}}{\beta_{ent}}} \right) \\ &= \frac{\gamma_{ent}}{\beta_{ent}} \sum_{\tau} \pi_{base} \ln \pi_{base} - \frac{p_c}{\beta_{ent}} + \ln \left(\frac{b_{\frac{\gamma_{ent}}{\beta_{ent}}} e^{1/\beta_{ent}}}{C(\pi_{ent})} \right). \end{aligned}$$

Substituting the expression for $1/\beta_{ent}$ leads to a relationship between divergence and correctness:

$$\begin{aligned} \mathbb{D}_{KL}(\pi_{base} \parallel \pi_{ent}) &= \frac{\gamma_{ent}}{\beta_{ent}} \sum_{\tau} \pi_{base} \ln \pi_{base} + p_c \ln b_{\frac{\gamma_{ent}}{\beta_{ent}}} + (1 - p_c) \ln(B_{\frac{\gamma_{ent}}{\beta_{ent}}} - b_{\frac{\gamma_{ent}}{\beta_{ent}}}) \\ &\quad - [p_c \ln C(\pi_{ent}) + (1 - p_c) \ln(1 - C(\pi_{ent}))]. \end{aligned}$$

Step 2: Analyze Differential Policy (π_{DS}). Similarly, the correctness is:

$$C(\pi_{DS}) = \frac{b_{\frac{\gamma_{DS}}{\beta_{DS}}} e^{1/\beta_{DS}}}{b_{\frac{\gamma_{DS}}{\beta_{DS}}} e^{1/\beta_{DS}} + (1 - p_c)}.$$

The reverse KL divergence, after a similar derivation, is:

$$\begin{aligned} \mathbb{D}_{KL}(\pi_{base} \parallel \pi_{DS}) &= \frac{\gamma_{DS}}{\beta_{DS}} \sum_{\tau \in \mathcal{C}} \pi_{base} \ln \pi_{base} + p_c \ln b_{\frac{\gamma_{DS}}{\beta_{DS}}} + (1 - p_c) \ln(1 - p_c) \\ &\quad - [p_c \ln C(\pi_{DS}) + (1 - p_c) \ln(1 - C(\pi_{DS}))]. \end{aligned} \tag{7}$$

Step 3: Compare the Policies. Our goal is to show that for any $C(\pi_{ent})$, we can choose parameters for our method to achieve $C(\pi_{DS}) = C(\pi_{ent})$ with a smaller or equal KL divergence. Let's choose $\gamma_{DS} = \frac{\beta_{DS}}{\beta_{ent}} \gamma_{ent}$, and set $C(\pi_{DS}) = C(\pi_{ent}) = C$. Equivalently, we assume that

$$\frac{\gamma_{DS}}{\beta_{DS}} = \frac{\gamma_{ent}}{\beta_{ent}} = \tilde{\gamma}.$$

Then the KL divergence for our method becomes:

$$\mathbb{D}_{KL}(\pi_{base} \parallel \pi_{DS}) = \tilde{\gamma} \sum_{\tau \in \mathcal{C}} \pi_{base} \ln \pi_{base} + p_c \ln b_{\gamma_{ent}} + (1 - p_c) \ln(1 - p_c) - H(C_{ent}),$$

where $H(C) = -[p_c \ln C + (1 - p_c) \ln(1 - C)]$. For the entropy method, the KL is:

$$\mathbb{D}_{\text{KL}}(\pi_{\text{base}} \parallel \pi_{\text{ent}}) = \tilde{\gamma} \sum_{\tau \in \mathcal{C}} \pi_{\text{base}} \ln \pi_{\text{base}} + \tilde{\gamma} \sum_{\tau \notin \mathcal{C}} \pi_{\text{base}} \ln \pi_{\text{base}} + p_c \ln b_{\tilde{\gamma}} + (1 - p_c) \ln(B_{\tilde{\gamma}} - b_{\tilde{\gamma}}) - H(C_{\text{ent}}).$$

The difference is $\mathbb{D}_{\text{KL}}(\pi_{\text{base}} \parallel \pi_{\text{ent}}) - \mathbb{D}_{\text{KL}}(\text{ours}) = \tilde{\gamma} \sum_{\tau \notin \mathcal{C}} \pi_{\text{base}} \ln \pi_{\text{base}} + (1 - p_c) \ln(B_{\tilde{\gamma}} - b_{\tilde{\gamma}}) - (1 - p_c) \ln(1 - p_c)$. By Jensen's inequality on the concave function $\ln(\cdot)$:

$$\sum_{\tau \notin \mathcal{C}} \frac{\pi_{\text{base}}(\tau)}{1 - p_c} \ln \left([\pi_{\text{base}}(\tau)]^{-\tilde{\gamma}} \right) \leq \ln \left(\sum_{\tau \notin \mathcal{C}} \frac{\pi_{\text{base}}(\tau)}{1 - p_c} [\pi_{\text{base}}(\tau)]^{-\tilde{\gamma}} \right) = \ln \left(\frac{B_{\tilde{\gamma}} - b_{\tilde{\gamma}}}{1 - p_c} \right)$$

Multiplying by $-(1 - p_c)$ gives:

$$\tilde{\gamma} \sum_{\tau \notin \mathcal{C}} \pi_{\text{base}}(\tau) \ln(\pi_{\text{base}}(\tau)) \geq -(1 - p_c) \ln \left(\frac{B_{\tilde{\gamma}} - b_{\tilde{\gamma}}}{1 - p_c} \right) = -(1 - p_c) \left[\ln(B_{\tilde{\gamma}} - b_{\tilde{\gamma}}) - \ln(1 - p_c) \right].$$

Therefore, the difference is non-negative: $\mathbb{D}_{\text{KL}}(\pi_{\text{base}} \parallel \pi_{\text{ent}}) - \mathbb{D}_{\text{KL}}(\pi_{\text{base}} \parallel \pi_{\text{DS}}) \geq 0$. This means that for any given correctness level C , our method (with $\gamma_{\text{DS}} = \gamma_{\text{ent}} \cdot \frac{\beta_{\text{DS}}}{\beta_{\text{ent}}}$) can achieve it with a lower or equal KL-divergence cost. Thus, if both methods are constrained by $\mathbb{D}_{\text{KL}}(\pi_{\text{base}} \parallel \pi_{\text{ent}}) \leq \kappa$ and $\mathbb{D}_{\text{KL}}(\pi_{\text{base}} \parallel \pi_{\text{DS}}) \leq \kappa$, our method can achieve a correctness $C(\pi_{\text{DS}}) \geq C(\pi_{\text{ent}})$. \square

Lemma B.7 (Correctness under Forward KL Constraint). *When $K_{\rho}(\pi, \pi_{\text{base}}) = \mathbb{D}_{\text{KL}}(\pi \parallel \pi_{\text{base}})$, for any $\gamma_{\text{ent}} \geq 0, \beta_{\text{ent}} > 0$ such that $\mathbb{D}_{\text{KL}}(\pi_{\text{ent}} \parallel \pi_{\text{base}}) \leq \kappa$, there exist $\gamma_{\text{DS}} \geq 0$ and $\beta_{\text{DS}} > 0$ such that $\mathbb{D}_{\text{KL}}(\pi_{\text{DS}} \parallel \pi_{\text{base}}) \leq \kappa$ and $C(\pi_{\text{DS}}) \geq C(\pi_{\text{ent}})$.*

Proof. The proof proceeds in three steps: we first find a functional relationship between correctness C and the KL divergence for each policy, and then compare them.

Step 1: Analyze the Entropy-Maximization Policy (π_{ent}). The correctness of π_{ent} is the total probability mass on correct trajectories:

$$C(\pi_{\text{ent}}) = \frac{\sum_{\tau \in \mathcal{C}} [\pi_{\text{base}}(\tau)]^{1 - \frac{\gamma_{\text{ent}}}{\beta_{\text{ent}}}} \exp(1/\beta_{\text{ent}})}{\sum_{\tau \in \mathcal{T}} [\pi_{\text{base}}(\tau)]^{1 - \frac{\gamma_{\text{ent}}}{\beta_{\text{ent}}}} \exp(r(\tau)/\beta_{\text{ent}})} = \frac{b_{\frac{\gamma_{\text{ent}}}{\beta_{\text{ent}}}} e^{1/\beta_{\text{ent}}}}{b_{\frac{\gamma_{\text{ent}}}{\beta_{\text{ent}}}} e^{1/\beta_{\text{ent}}} + (B_{\frac{\gamma_{\text{ent}}}{\beta_{\text{ent}}}} - b_{\frac{\gamma_{\text{ent}}}{\beta_{\text{ent}}}})}. \quad (8)$$

Solving for $e^{1/\beta_{\text{ent}}}$ yields: $e^{1/\beta_{\text{ent}}} = \frac{B_{\frac{\gamma_{\text{ent}}}{\beta_{\text{ent}}}} - b_{\frac{\gamma_{\text{ent}}}{\beta_{\text{ent}}}}}{b_{\frac{\gamma_{\text{ent}}}{\beta_{\text{ent}}}}} \left(\frac{C(\pi_{\text{ent}})}{1 - C(\pi_{\text{ent}})} \right)$.

The reverse KL divergence $\mathbb{D}_{\text{KL}}(\pi_{\text{ent}} \parallel \pi_{\text{base}})$ can be expressed as a function of $C(\pi_{\text{ent}})$. Following the derivation previously, we arrive at:

$$\begin{aligned} \mathbb{D}_{\text{KL}}(\pi_{\text{ent}} \parallel \pi_{\text{base}}) &= -\frac{\frac{\gamma_{\text{ent}}}{\beta_{\text{ent}}}}{b_{\frac{\gamma_{\text{ent}}}{\beta_{\text{ent}}}}} \sum_{\tau \in \mathcal{C}} \pi_{\text{base}}(\tau)^{1 - \frac{\gamma_{\text{ent}}}{\beta_{\text{ent}}}} \ln(\pi_{\text{base}}(\tau)) \cdot C(\pi_{\text{ent}}) \\ &\quad - \frac{\frac{\gamma_{\text{ent}}}{\beta_{\text{ent}}}}{B_{\frac{\gamma_{\text{ent}}}{\beta_{\text{ent}}}} - b_{\frac{\gamma_{\text{ent}}}{\beta_{\text{ent}}}}} \sum_{\tau \notin \mathcal{C}} \pi_{\text{base}}(\tau)^{1 - \frac{\gamma_{\text{ent}}}{\beta_{\text{ent}}}} \ln(\pi_{\text{base}}(\tau)) \cdot (1 - C(\pi_{\text{ent}})) \\ &\quad + (1 - C(\pi_{\text{ent}})) \ln \left(\frac{b_{\frac{\gamma_{\text{ent}}}{\beta_{\text{ent}}}}}{B_{\frac{\gamma_{\text{ent}}}{\beta_{\text{ent}}}} - b_{\frac{\gamma_{\text{ent}}}{\beta_{\text{ent}}}}} \right) - \ln b_{\frac{\gamma_{\text{ent}}}{\beta_{\text{ent}}}} + H(C(\pi_{\text{ent}})), \end{aligned} \quad (9)$$

where $H(C) = C \ln C + (1 - C) \ln(1 - C)$ is the binary entropy function.

Step 2: Analyze Differential Policy (π_{DS}). Similarly, the correctness for our policy is given by:

$$C(\pi_{\text{DS}}) = \frac{b_{\frac{\gamma_{\text{DS}}}{\beta_{\text{DS}}}} e^{1/\beta_{\text{DS}}}}{b_{\frac{\gamma_{\text{DS}}}{\beta_{\text{DS}}}} e^{1/\beta_{\text{DS}}} + (1 - p_c)}. \quad (10)$$

The corresponding reverse KL divergence as a function of $C(\pi_{\text{DS}})$ is:

$$\begin{aligned} \mathbb{D}_{\text{KL}}(\pi_{\text{DS}}\|\pi_{\text{base}}) &= -\frac{\frac{\gamma_{\text{DS}}}{\beta_{\text{DS}}}}{b\frac{\gamma_{\text{DS}}}{\beta_{\text{DS}}}} \sum_{\tau \in \mathcal{C}} \pi_{\text{base}}(\tau)^{1-\frac{\gamma_{\text{DS}}}{\beta_{\text{DS}}}} \ln(\pi_{\text{base}}(\tau)) \cdot C(\pi_{\text{DS}}) \\ &\quad + (1 - C(\pi_{\text{DS}})) \ln \left(\frac{b\frac{\gamma_{\text{DS}}}{\beta_{\text{DS}}}}{1 - p_c} \right) - \ln b\frac{\gamma_{\text{DS}}}{\beta_{\text{DS}}} + H(C(\pi_{\text{DS}})). \end{aligned} \quad (11)$$

Step 3: Compare the Policies. Our goal is to show that for any $C(\pi_{\text{ent}})$, we can choose parameters for our method to achieve $C(\pi_{\text{DS}}) = C(\pi_{\text{ent}})$ with a smaller or equal KL divergence. Let's choose $\gamma_{\text{DS}} = \frac{\beta_{\text{DS}}}{\beta_{\text{ent}}} \gamma_{\text{ent}}$, and set $C(\pi_{\text{DS}}) = C(\pi_{\text{ent}}) = C$. Equivalently, we assume that

$$\frac{\gamma_{\text{DS}}}{\beta_{\text{DS}}} = \frac{\gamma_{\text{ent}}}{\beta_{\text{ent}}} = \tilde{\gamma}.$$

Then the KL divergence for our method becomes: According to Jensen's inequality, we have

$$\frac{\tilde{\gamma} \sum_{\tau \notin \mathcal{C}} \pi_{\text{base}}(\tau)^{1-\tilde{\gamma}} \ln(\pi_{\text{base}}(\tau))}{B_{\tilde{\gamma}} - b_{\tilde{\gamma}}} \cdot (1 - C) \leq (1 - C) \cdot \ln \left(\frac{\sum_{\tau \notin \mathcal{C}} \pi_{\text{base}}(\tau)}{B_{\tilde{\gamma}} - b_{\tilde{\gamma}}} \right) = (1 - C) \cdot \ln \left(\frac{1 - p_C}{B_{\tilde{\gamma}} - b_{\tilde{\gamma}}} \right)$$

Then in this case we have

$$\begin{aligned} \mathbb{D}_{\text{KL}}(\pi_{\text{ent}}\|\pi_{\text{base}}) &= -\frac{\tilde{\gamma} \cdot \sum_{\tau \in \mathcal{C}} \pi_{\text{base}}(\tau)^{1-\tilde{\gamma}} \ln(\pi_{\text{base}}(\tau))}{b_{\tilde{\gamma}}} \cdot C + (1 - C) \left[\ln \left(\frac{b_{\tilde{\gamma}}}{B_{\tilde{\gamma}} - b_{\tilde{\gamma}}} \right) \right] - \ln b_{\tilde{\gamma}} \\ &\quad + C \ln C + (1 - C) \ln(1 - C) - \frac{\tilde{\gamma} \sum_{\tau \notin \mathcal{C}} \pi_{\text{base}}(\tau)^{1-\tilde{\gamma}} \ln(\pi_{\text{base}}(\tau))}{1 - p_C} \cdot (1 - C) \\ &\geq -\frac{\tilde{\gamma} \sum_{\tau \in \mathcal{C}} \pi_{\text{base}}(\tau)^{1-\tilde{\gamma}} \ln(\pi_{\text{base}}(\tau))}{b_{\tilde{\gamma}}} \cdot C + (1 - C) \left[\ln \left(\frac{b_{\tilde{\gamma}}}{B_{\tilde{\gamma}} - b_{\tilde{\gamma}}} \right) \right] - \ln b_{\tilde{\gamma}} \\ &\quad + C \ln C + (1 - C) \ln(1 - C) \\ &= \mathbb{D}_{\text{KL}}(\pi_{\text{DS}}\|\pi_{\text{base}}) \end{aligned}$$

Therefore, the difference is non-negative: $\mathbb{D}_{\text{KL}}(\pi_{\text{ent}}\|\pi_{\text{base}}) - \mathbb{D}_{\text{KL}}(\pi_{\text{DS}}\|\pi_{\text{base}}) \geq 0$. This means that for any given correctness level C , our method (with $\gamma_{\text{DS}} = \gamma_{\text{ent}} \cdot \frac{\beta_{\text{DS}}}{\beta_{\text{ent}}}$) can achieve it with a lower or equal KL-divergence cost. Thus, if the entropy method is constrained by $\mathbb{D}_{\text{KL}} \leq \kappa$, our method can achieve a correctness $C(\pi_{\text{DS}}) \geq C(\pi_{\text{ent}})$ while also satisfying the constraint. \square

Lemma B.8 (Correctness under Reverse χ^2 Constraint). *When $K_{\rho}(\pi, \pi_{\text{base}}) = \mathbb{D}_{\chi^2}(\pi_{\text{base}}\|\pi)$, for any $\gamma_{\text{ent}} \geq 0, \beta_{\text{ent}} > 0$ such that $\mathbb{D}_{\text{KL}}(\pi_{\text{base}}\|\pi_{\text{ent}}) \leq \kappa$, there exist $\gamma_{\text{DS}} \geq 0$ and $\beta_{\text{DS}} > 0$ such that $\mathbb{D}_{\chi^2}(\pi_{\text{base}}\|\pi_{\text{DS}}) \leq \kappa$ and $C(\pi_{\text{DS}}) \geq C(\pi_{\text{ent}})$.*

Step 1: Analyze the Entropy-Maximization Policy (π_{ent}). The correctness of π_{ent} is the total probability mass on correct trajectories:

$$C(\pi_{\text{ent}}) = \frac{\sum_{\tau \in \mathcal{C}} [\pi_{\text{base}}(\tau)]^{1-\frac{\gamma_{\text{ent}}}{\beta_{\text{ent}}}} \exp(1/\beta_{\text{ent}})}{\sum_{\tau \in \mathcal{T}} [\pi_{\text{base}}(\tau)]^{1-\frac{\gamma_{\text{ent}}}{\beta_{\text{ent}}}} \exp(r(\tau)/\beta_{\text{ent}})} = \frac{b\frac{\gamma_{\text{ent}}}{\beta_{\text{ent}}} e^{1/\beta_{\text{ent}}}}{b\frac{\gamma_{\text{ent}}}{\beta_{\text{ent}}} e^{1/\beta_{\text{ent}}} + (B\frac{\gamma_{\text{ent}}}{\beta_{\text{ent}}} - b\frac{\gamma_{\text{ent}}}{\beta_{\text{ent}}})}. \quad (12)$$

Solving for $e^{1/\beta_{\text{ent}}}$ yields: $e^{1/\beta_{\text{ent}}} = \frac{B\frac{\gamma_{\text{ent}}}{\beta_{\text{ent}}} - b\frac{\gamma_{\text{ent}}}{\beta_{\text{ent}}}}{b\frac{\gamma_{\text{ent}}}{\beta_{\text{ent}}}} \left(\frac{C(\pi_{\text{ent}})}{1 - C(\pi_{\text{ent}})} \right)$.

The reverse χ^2 divergence $\mathbb{D}_{\chi^2}(\pi_{\text{base}}\|\pi_{\text{ent}})$ can be expressed as a function of $C(\pi_{\text{ent}})$. Following the derivation previously, we arrive at:

$$\mathbb{D}_{\chi^2}(\pi_{\text{base}}\|\pi_{\text{ent}}) = \sum_{\tau} \pi_{\text{base}}(\tau) \left(\frac{\pi_{\text{ent}}(\tau)}{\pi_{\text{base}}(\tau)} - 1 \right)^2 = \sum_{\tau} \frac{(\pi_{\text{ent}}(\tau))^2}{\pi_{\text{base}}(\tau)} - 1$$

We insert the expression of π_{ent} into the divergence constraints and we can obtain that

$$\mathbb{D}_{\chi^2}(\pi_{\text{base}}\|\pi_{\text{ent}}) = -1 + \frac{e^{\frac{2}{\beta_{\text{ent}}}} \sum_{\tau \in \mathcal{C}} \pi_{\text{base}}(\tau)^{1-2\frac{\gamma_{\text{ent}}}{\beta_{\text{ent}}}} + \sum_{\tau \notin \mathcal{C}} \pi_{\text{base}}(\tau)^{1-2\frac{\gamma_{\text{ent}}}{\beta_{\text{ent}}}}}{\left[B_{\frac{\gamma_{\text{ent}}}{\beta_{\text{ent}}}} - b_{\frac{\gamma_{\text{ent}}}{\beta_{\text{ent}}}} + b_{\frac{\gamma_{\text{ent}}}{\beta_{\text{ent}}}} e^{\frac{1}{\beta_{\text{ent}}}} \right]^2}$$

We then insert Eq. 12 into the expression of divergence and we can obtain that

$$\mathbb{D}_{\chi^2}(\pi_{\text{base}}\|\pi_{\text{ent}}) = -1 + \frac{\sum_{\tau \in \mathcal{C}} \pi_{\text{base}}(\tau)^{1-2\frac{\gamma_{\text{ent}}}{\beta_{\text{ent}}}}}{b_{\frac{\gamma_{\text{ent}}}{\beta_{\text{ent}}}}^2} \cdot C(\pi_{\text{ent}})^2 + (1 - C(\pi_{\text{ent}}))^2 \frac{\sum_{\tau \notin \mathcal{C}} \pi_{\text{base}}(\tau)^{1-2\frac{\gamma_{\text{ent}}}{\beta_{\text{ent}}}}}{\left(B_{\frac{\gamma_{\text{ent}}}{\beta_{\text{ent}}}} - b_{\frac{\gamma_{\text{ent}}}{\beta_{\text{ent}}}} \right)^2}$$

Step 2: Analyze Differential Policy (π_{DS}). Similarly, the correctness is:

$$C(\pi_{\text{DS}}) = \frac{b_{\frac{\gamma_{\text{DS}}}{\beta_{\text{DS}}}} e^{1/\beta_{\text{DS}}}}{b_{\frac{\gamma_{\text{DS}}}{\beta_{\text{DS}}}} e^{1/\beta_{\text{DS}}} + (1 - p_c)}.$$

The reverse χ^2 divergence, after a similar derivation, is:

$$\mathbb{D}_{\chi^2}(\pi_{\text{base}}\|\pi_{\text{DS}}) = -1 + \frac{\sum_{\tau \in \mathcal{C}} \pi_{\text{base}}(\tau)^{1-2\frac{\gamma_{\text{DS}}}{\beta_{\text{DS}}}}}{b_{\frac{\gamma_{\text{DS}}}{\beta_{\text{DS}}}}^2} \cdot C(\pi_{\text{DS}})^2 + (1 - C(\pi_{\text{DS}}))^2 \frac{\sum_{\tau \notin \mathcal{C}} \pi_{\text{base}}(\tau)}{(1 - p_c)^2}$$

Step 3: Compare the Policies. Our goal is to show that for any $C(\pi_{\text{ent}})$, we can choose parameters for our method to achieve $C(\pi_{\text{DS}}) \geq C(\pi_{\text{ent}})$ with a smaller or equal χ^2 divergence. Let's choose $\gamma_{\text{DS}} = \frac{\beta_{\text{DS}}}{\beta_{\text{ent}}}\gamma_{\text{ent}}$, and set $C(\pi_{\text{DS}}) = C(\pi_{\text{ent}}) = C$. Equivalently, we assume that

$$\frac{\gamma_{\text{DS}}}{\beta_{\text{DS}}} = \frac{\gamma_{\text{ent}}}{\beta_{\text{ent}}} = \tilde{\gamma}.$$

According to Cauchy Inequality:

$$\left[\sum_{\tau \notin \mathcal{C}} \pi_{\text{base}}(\tau)^{1-2\tilde{\gamma}} \right] \cdot \left[\sum_{\tau \notin \mathcal{C}} \pi_{\text{base}}(\tau) \right] \geq \left[\sum_{\tau \notin \mathcal{C}} \pi_{\text{base}}(\tau)^{1-\tilde{\gamma}} \right]^2.$$

Thus, we have

$$\begin{aligned} \mathbb{D}_{\chi^2}(\pi_{\text{base}}\|\pi_{\text{ent}}) &= -1 + \frac{\sum_{\tau \in \mathcal{C}} \pi_{\text{base}}(\tau)^{1-2\tilde{\gamma}}}{b_{\tilde{\gamma}}^2} \cdot C(\pi_{\text{ent}})^2 + (1 - C(\pi_{\text{ent}}))^2 \frac{\sum_{\tau \notin \mathcal{C}} \pi_{\text{base}}(\tau)^{1-2\tilde{\gamma}}}{\left(B_{\tilde{\gamma}} - b_{\tilde{\gamma}} \right)^2} \\ &\geq -1 + \frac{\sum_{\tau \in \mathcal{C}} \pi_{\text{base}}(\tau)^{1-2\tilde{\gamma}}}{b_{\tilde{\gamma}}^2} \cdot C(\pi_{\text{ent}})^2 + (1 - C(\pi_{\text{ent}}))^2 \frac{1}{\sum_{\tau \notin \mathcal{C}} \pi_{\text{base}}(\tau)} = \mathbb{D}_{\chi^2}(\pi_{\text{base}}\|\pi_{\text{DS}}). \end{aligned}$$

Therefore, the difference is non-negative: $\mathbb{D}_{\chi^2}(\pi_{\text{base}}\|\pi_{\text{ent}}) - \mathbb{D}_{\chi^2}(\pi_{\text{base}}\|\pi_{\text{DS}}) \geq 0$. This means that for any given correctness level C , our method (with $\gamma_{\text{DS}} = \gamma_{\text{ent}} \cdot \frac{\beta_{\text{DS}}}{\beta_{\text{ent}}}$) can achieve it with a lower or equal KL-divergence cost. Thus, if both methods are constrained by $\mathbb{D}_{\text{KL}}(\pi_{\text{base}}\|\pi_{\text{ent}}) \leq \kappa$ and $\mathbb{D}_{\text{KL}}(\pi_{\text{base}}\|\pi_{\text{DS}}) \leq \kappa$, our method can achieve a correctness $C(\pi_{\text{DS}}) \geq C(\pi_{\text{ent}})$.

Lemma B.9 (Correctness under Forward χ^2 Constraint). *When $K_{\rho}(\pi, \pi_{\text{base}}) = \mathbb{D}_{\chi^2}(\pi\|\pi_{\text{base}})$, for any $\gamma_{\text{ent}} \geq 0, \beta_{\text{ent}} > 0$ such that $\mathbb{D}_{\chi^2}(\pi_{\text{ent}}\|\pi_{\text{base}}) \leq \kappa$, there exist $\gamma_{\text{DS}} \geq 0$ and $\beta_{\text{DS}} > 0$ such that $\mathbb{D}_{\chi^2}(\pi_{\text{DS}}\|\pi_{\text{base}}) \leq \kappa$ and $C(\pi_{\text{DS}}) \geq C(\pi_{\text{ent}})$.*

Proof. The proof proceeds in three steps: we first find a functional relationship between correctness C and the KL divergence for each policy, and then compare them.

Step 1: Analyze the Entropy-Maximization Policy (π_{ent}). The correctness of π_{ent} is the total probability mass on correct trajectories:

$$C(\pi_{\text{ent}}) = \frac{\sum_{\tau \in \mathcal{C}} [\pi_{\text{base}}(\tau)]^{1-\frac{\gamma_{\text{ent}}}{\beta_{\text{ent}}}} \exp(1/\beta_{\text{ent}})}{\sum_{\tau \in \mathcal{T}} [\pi_{\text{base}}(\tau)]^{1-\frac{\gamma_{\text{ent}}}{\beta_{\text{ent}}}} \exp(r(\tau)/\beta_{\text{ent}})} = \frac{b_{\frac{\gamma_{\text{ent}}}{\beta_{\text{ent}}}} e^{1/\beta_{\text{ent}}}}{b_{\frac{\gamma_{\text{ent}}}{\beta_{\text{ent}}}} e^{1/\beta_{\text{ent}}} + (B_{\frac{\gamma_{\text{ent}}}{\beta_{\text{ent}}}} - b_{\frac{\gamma_{\text{ent}}}{\beta_{\text{ent}}}})}. \quad (13)$$

Solving for $e^{1/\beta_{\text{ent}}}$ yields: $e^{1/\beta_{\text{ent}}} = \frac{B_{\frac{\gamma_{\text{ent}}}{\beta_{\text{ent}}}} - b_{\frac{\gamma_{\text{ent}}}{\beta_{\text{ent}}}}}{b_{\frac{\gamma_{\text{ent}}}{\beta_{\text{ent}}}}} \left(\frac{C(\pi_{\text{ent}})}{1 - C(\pi_{\text{ent}})} \right)$.

The reverse χ^2 divergence $\mathbb{D}_{\chi^2}(\pi_{\text{ent}} \parallel \pi_{\text{base}})$ can be expressed as a function of $C(\pi_{\text{ent}})$. Following the derivation previously, we arrive at:

$$\begin{aligned} \mathbb{D}_{\chi^2}(\pi_{\text{ent}} \parallel \pi_{\text{base}}) &= -1 + \left[\sum_{\tau} \pi_{\text{base}}(\tau)^{1-\frac{\gamma_{\text{ent}}}{\beta_{\text{ent}}}} \exp\left(\frac{r(\tau)}{\beta_{\text{ent}}}\right) \right] \cdot \left[\sum_{\tau} \pi_{\text{base}}(\tau)^{1+\frac{\gamma_{\text{ent}}}{\beta_{\text{ent}}}} \exp\left(-\frac{r(\tau)}{\beta_{\text{ent}}}\right) \right] \\ &= \frac{1}{C(\pi_{\text{ent}})} b_{\frac{\gamma_{\text{ent}}}{\beta_{\text{ent}}}} \sum_{\tau \in \mathcal{C}} \pi_{\text{base}}(\tau)^{1+\frac{\gamma_{\text{ent}}}{\beta_{\text{ent}}}} + \frac{1}{1 - C(\pi_{\text{ent}})} (B_{\frac{\gamma_{\text{ent}}}{\beta_{\text{ent}}}} - b_{\frac{\gamma_{\text{ent}}}{\beta_{\text{ent}}}}) \sum_{\tau \notin \mathcal{C}} \pi_{\text{base}}(\tau)^{1-\frac{\gamma_{\text{ent}}}{\beta_{\text{ent}}}} \end{aligned}$$

Step 2: Analyze Differential Policy (π_{DS}). Similarly, the correctness for our policy is given by:

$$C(\pi_{\text{DS}}) = \frac{b_{\frac{\gamma_{\text{DS}}}{\beta_{\text{DS}}}} e^{1/\beta_{\text{DS}}}}{b_{\frac{\gamma_{\text{DS}}}{\beta_{\text{DS}}}} e^{1/\beta_{\text{DS}}} + (1 - p_c)}. \quad (14)$$

The corresponding reverse χ^2 divergence as a function of $C(\pi_{\text{DS}})$ is:

$$\mathbb{D}_{\chi^2}(\pi_{\text{ent}} \parallel \pi_{\text{base}}) = \frac{1}{C(\pi_{\text{ent}})} b_{\frac{\gamma_{\text{DS}}}{\beta_{\text{DS}}}} \sum_{\tau \in \mathcal{C}} \pi_{\text{base}}(\tau)^{1+\frac{\gamma_{\text{DS}}}{\beta_{\text{DS}}}} + \frac{1}{(1 - C(\pi_{\text{ent}}))} ((1 - p_c)) \sum_{\tau \notin \mathcal{C}} \pi_{\text{base}}(\tau)^{1+\frac{\gamma_{\text{DS}}}{\beta_{\text{DS}}}}$$

Step 3: Compare the Policies. Our goal is to show that for any $C(\pi_{\text{ent}})$, we can choose parameters for our method to achieve $C(\pi_{\text{DS}}) \geq C(\pi_{\text{ent}})$ with a smaller or equal χ^2 divergence. Let's choose $\gamma_{\text{DS}} = \frac{\beta_{\text{DS}}}{\beta_{\text{ent}}} \gamma_{\text{ent}}$, and set $C(\pi_{\text{DS}}) = C(\pi_{\text{ent}}) = C$. Equivalently, we assume that

$$\frac{\gamma_{\text{DS}}}{\beta_{\text{DS}}} = \frac{\gamma_{\text{ent}}}{\beta_{\text{ent}}} = \tilde{\gamma}.$$

. According to Cauchy Inequality:

$$\left[\sum_{\tau \notin \mathcal{C}} \pi_{\text{base}}(\tau)^{1+\tilde{\gamma}} \right] \cdot \left[\sum_{\tau \notin \mathcal{C}} \pi_{\text{base}}(\tau)^{1-\tilde{\gamma}} \right] \geq \left[\sum_{\tau \notin \mathcal{C}} \pi_{\text{base}}(\tau) \right]^2.$$

Thus, we have

$$\begin{aligned} \mathbb{D}_{\chi^2}(\pi_{\text{ent}} \parallel \pi_{\text{base}}) &= \frac{1}{C(\pi_{\text{ent}})} b_{\tilde{\gamma}} \sum_{\tau \in \mathcal{C}} \pi_{\text{base}}(\tau)^{1+\tilde{\gamma}} + \frac{1}{1 - C(\pi_{\text{ent}})} (B_{\tilde{\gamma}} - b_{\tilde{\gamma}}) \sum_{\tau \notin \mathcal{C}} \pi_{\text{base}}(\tau)^{1-\tilde{\gamma}} \\ &\geq \frac{1}{C(\pi_{\text{ent}})} b_{\tilde{\gamma}} \sum_{\tau \in \mathcal{C}} \pi_{\text{base}}(\tau)^{1+\tilde{\gamma}} + \frac{1}{1 - C(\pi_{\text{ent}})} \left(\sum_{\tau \notin \mathcal{C}} \pi_{\text{base}}(\tau) \right)^2 = \mathbb{D}_{\chi^2}(\pi_{\text{ent}} \parallel \pi_{\text{base}}) \end{aligned}$$

Therefore, the difference is non-negative: $\mathbb{D}_{\chi^2}(\pi_{\text{ent}} \parallel \pi_{\text{base}}) - \mathbb{D}_{\chi^2}(\pi_{\text{DS}} \parallel \pi_{\text{base}}) \geq 0$. This means that for any given correctness level C , our method (with $\gamma_{\text{DS}} = \gamma_{\text{ent}} \cdot \frac{\beta_{\text{DS}}}{\beta_{\text{ent}}}$) can achieve it with a lower or equal KL-divergence cost. Thus, if the entropy method is constrained by $\mathbb{D}_{\chi^2} \leq \kappa$, our method can achieve a correctness $C(\pi_{\text{DS}}) \geq C(\pi_{\text{ent}})$ while also satisfying the constraint. \square

Theorem B.10. *Assume the reward mechanism has access to all correct trajectories. For any parameters $\gamma_{ent} \geq 0$ and $\beta_{ent} > 0$ used in the entropy-regularized policy π_{ent} that satisfy a proximity constraint $K_\rho(\pi_{ent}, \pi_{base}) \leq \kappa$, there exist parameters $\gamma_{DS} \geq 0$ and $\beta_{n,p} > 0$ for our proposed policy π_{DS} such that it also satisfies $K_\rho(\pi_{DS}, \pi_{base}) \leq \kappa$, and the following inequalities hold:*

$$C(\pi_{DS}) \geq C(\pi_{ent}) \quad \text{and} \quad \sigma_{DS} \geq \sigma_{En}.$$

This result holds for divergence measures $K_\rho(\pi, \pi_{base})$ including $\mathbb{D}_{KL}(\pi \parallel \pi_{base})$, $\mathbb{D}_{KL}(\pi_{base} \parallel \pi)$, $\mathbb{D}_{\chi^2}(\pi \parallel \pi_{base})$, and $\mathbb{D}_{\chi^2}(\pi_{base} \parallel \pi)$.

Proof. According to Lemma B.6, Lemma B.7, Lemma B.8, and Lemma B.9, we obtain that Theorem B.10 holds for $K_\rho(\pi, \pi_{base}) = \mathbb{D}_{KL}(\pi \parallel \pi_{base})$, $\mathbb{D}_{KL}(\pi_{base} \parallel \pi)$, $\mathbb{D}_{\chi^2}(\pi \parallel \pi_{base})$, $\mathbb{D}_{\chi^2}(\pi_{base} \parallel \pi)$. Thus, we finish the proof of the theorem. \square

B.3 Equivalence of Theoretical and Practical Reward Modifications

In this section, we clarify the relationship between our theoretical reward modification and its practical implementation. Specifically, we demonstrate that subtracting a $\log \pi$ term from the reward is equivalent to subtracting a $\log \pi_{base}$ term, under a re-parameterization of the optimization objective.

Consider the following theoretical reward modification, which uses the policy's own probability π :

$$r_{DS}^\pi(\tau) = \begin{cases} r(\tau) - \gamma_p \cdot \log(\pi(\tau)) & \text{if } r(\tau) > 0 \quad (\text{correct trajectories}) \\ r(\tau) + \gamma_n \cdot \log(\pi(\tau)) & \text{if } r(\tau) \leq 0 \quad (\text{incorrect trajectories}). \end{cases} \quad (15)$$

We first define the theoretical optimization problem for parameters $\beta, \gamma_n, \gamma_p$:

$$\pi_{DS} = \arg \max_{\pi} \mathbb{E}_{\tau \sim \pi} [r_{DS}^\pi(\tau)] - \beta \cdot \mathbb{D}_{KL}(\pi \parallel \pi_{base}). \quad (16)$$

Now, consider an alternative formulation where the reward is modified using the base policy π_{base} :

$$r_{DS}^{\pi_{base}}(\tau) = \begin{cases} r(\tau) - \tilde{\gamma}_p \cdot \log(\pi_{base}(\tau)) & \text{if } r(\tau) > 0 \quad (\text{correct trajectories}) \\ r(\tau) + \tilde{\gamma}_n \cdot \log(\pi_{base}(\tau)) & \text{if } r(\tau) \leq 0 \quad (\text{incorrect trajectories}). \end{cases} \quad (17)$$

We show that the solution π_{DS} to the original problem (16) is **also** the solution to the following practical objective, which uses $r_{DS}^{\pi_{base}}$:

$$\pi_{DS} = \arg \max_{\pi} \mathbb{E}_{\tau \sim \pi} [r_{DS}^{\pi_{base}}(\tau)] - \tilde{\beta} \cdot \mathbb{D}_{KL}(\pi \parallel \pi_{base}). \quad (18)$$

This equivalence holds when the new parameters $\tilde{\beta}, \tilde{\gamma}_p$, and $\tilde{\gamma}_n$ are set as follows:

$$\tilde{\beta} = \beta + \gamma_p, \quad \tilde{\gamma}_p = \gamma_p, \quad \tilde{\gamma}_n = \frac{\gamma_n(\beta + \gamma_p)}{\beta + \gamma_n}. \quad (19)$$

Therefore, the theoretical analysis from Theorem 3.4 still holds when $\log \pi$ is substituted for $\log \pi_{base}$. Furthermore, the policy selection mechanism in Eq. 4 is equivalent to directly maximizing entropy via an added regularization term. In practice, we find that using $\log \pi_{\theta_{old}}$ (i.e., the log-probability of a previous policy iteration) in the advantage function modification yields empirically better performance than using $\log \pi_{base}$ (the log-probability of the base policy).

C Experimental Details

In this section, we provide additional details for the experiments in Section 4.

C.1 Countdown Experiment

C.1.1 Data

We use the dataset released by Pan et al. (2025), which contains 327,680 training samples and 1,024 test samples.¹ An example training prompt is shown below.

Countdown Task Example

[INST] Using the numbers [5, 94, 9, 44], create an equation that equals 93. You can use basic arithmetic operations (+, -, *, /) and each number can only be used once. Show your work in <think></think> tags. And return the final answer in <answer></answer> tags, for example <answer>(1 + 2) / 3</answer>. **[/INST]**

Let me solve this step by step.

Our implementation builds on the official repository of Pan et al. (2025)² and a fork adapted for A100 training.³

C.1.2 Training

We train with a global batch size of 128, with 5 rollouts per prompt, and use a mini-batch size of 64. The learning rate is 1×10^{-6} , and the KL penalty coefficient is set to $\beta_{\text{KL}} = 1 \times 10^{-3}$. The reward is 1 for correct responses, 0.1 for incorrect yet properly formatted responses, and 0 for all others. The maximum response length is 8,192 tokens. We perform RL fine-tuning of the Qwen2.5-3B-Instruct model (Qwen Team, 2024) for 320 steps on 2 A100 GPUs.

Table 2: Configuration for Qwen3-1.7B

Parameter	Value	Parameter	Value
Pretrained model	Qwen3-1.7B	Training set	DAPO14k
Prompts per batch	32	Generations per prompt	8
Gradient update per RL step	2	Max prompt length	1024
Max response length	4096	Learning rate	5×10^{-7}
Clip ratio low	0.2	Clip ratio high	0.25
Training Steps	300	β	0.0
Entropy coefficient	0.0	γ_p	0.02
γ_n	0.002	Remove padding	Enabled
Rollout engine	v11m	Rollout temperature	0.7
Validation temperature	0.7	Device	4 x Nvidia-H100

For Qwen2.5-Math-7B model, we trained for three random seeds. During evaluation, we first generated 128 rollouts for each question, then estimated Pass@1 to Pass@64 using the unbiased estimator of each metric respectively, following Walder & Karkhanis (2025b).

C.2 Baseline Implementation

GR-PKPO. We attempted to train the model using the Pass@ k metric directly as the reward signal for $k \in \{2, 3, 4\}$. However, this approach proved unstable across all configurations. The training process quickly collapsed, causing the model to generate degenerate outputs and yielding performance substantially worse than the baseline. Consequently, these results are omitted from our main comparisons. We hypothesize this instability may be attributed to the limited number of rollouts (5) used during training.

¹<https://huggingface.co/datasets/Jiayi-Pan/Countdown-Tasks-3to4>

²<https://github.com/Jiayi-Pan/TinyZero>

³<https://github.com/JerryWu-code/TinyZero>

Table 3: Configuration for Qwen2.5-Math-1.5B

Parameter	Value	Parameter	Value
Pretrained Model	Qwen2.5-Math-1.5B	Training Set	DAPO14k + MATH12k
Prompts per batch	32	Generations per prompt	8
Gradient update per RL step	1	Max prompt length	1024
Max response length	2048	Learning rate	1×10^{-6}
Clip ratio low	0.2	Clip ratio high	0.25
Training Steps	1000	β	0.0
Entropy coefficient	0.0	γ_p	0.01
γ_n	0.01	Remove padding	Enabled
Rollout engine	v11m	Rollout temperature	0.7
Validation temperature	0.7	Device	4 x Nvidia-L6000

Table 4: Configuration for Qwen2.5-Math-7B

Parameter	Value	Parameter	Value
Pretrained Model	Qwen2.5-Math-7B	Training Set	DAPO14k + MATH12k
Prompts per batch	32	Generations per prompt	8
Gradient update per RL step	1	Max prompt length	1024
Max response length	2048	Learning rate	1×10^{-6}
Clip ratio low	0.2	Clip ratio high	0.25
Training Steps	500	β	0.0
Entropy coefficient	0.0	γ_p	0.01
γ_n	0.01	Remove padding	Enabled
Rollout engine	v11m	Rollout temperature	0.7
Validation temperature	0.7	Device	4 x Nvidia-A100

Unlikeliness Reward Method. We compare against the rank-based penalty proposed by He et al. (2025a), which down-weights the reward for high-probability solutions to encourage diversity. For a set of rollouts $\{y_i\}_{i=1}^G$, the modified reward is:

$$r_{\text{unlikely}}(y_i) = r(y_i) \left(1 - \beta_{\text{rank}} \frac{G - \text{rank}(y_i)}{G} \right),$$

where $\text{rank}(y_i)$ is the rank of the solution y_i based on its probability under the policy $\pi_{\text{old}}(\cdot \mid x)$. We performed a hyperparameter sweep for $\beta_{\text{rank}} \in \{0.05, 0.1, 0.15, 0.2, 0.25, 0.3\}$ and found that $\beta_{\text{rank}} = 0.05$ yielded the best Pass@64 performance. For values of $\beta_{\text{rank}} \geq 0.15$, the training became unstable and collapsed.

Entropy-Based Methods. For the entropy-based baselines, we augment GRPO with either an entropy bonus or penalty. We swept the coefficients η_+ and η_- over the set $\{0.005, 0.01, 0.03, 0.05\}$. In Figure 4, we report the results for the hyperparameter value that achieved the highest Pass@64 score. A comprehensive summary of all experimental runs is available in Appendix D.

C.3 Math Reasoning Experiment

We first filter out 14,042 questions that are written in English from the DAPO dataset (Yu et al., 2025), and combined them with 11,998 questions in the MATH12k dataset (Hendrycks et al., 2021). After that, we conduct reinforcement finetuning on Qwen2.5-Math-1.5B (Qwen Team, 2024), Qwen3-1.7B (Qwen Team, 2025) and Minstral-8B-Instruct (Jiang et al., 2024) model. The detailed training setups are shown in Tab. 756, and response examples are shown in boxes below respectively.

Table 5: Configuration for Minstral-8B-Instruct

Parameter	Value	Parameter	Value
Pretrained model	Minstral-8B-Instruct	Training set	DAPO14k + MATH12k
Prompts per batch	32	Generations per prompt	8
Gradient update per RL step	2	Max prompt length	1024
Max response length	2048	Learning rate	3×10^{-7}
Clip ratio low	0.2	Clip ratio high	0.22
Training steps	300	β	0.001
Entropy coefficient	0.0	γ_p	0.02
γ_n	0.002	Remove padding	Enabled
Rollout engine	v1lm	Rollout temperature	0.7
Validation temperature	0.7	Device	4 x Nvidia-A100

Mistral Instruction Response Example

[INST] Convert the point $(0, 3)$ in rectangular coordinates to polar coordinates. Enter your answer in the form (r, θ) , where $r > 0$ and $0 \leq \theta < 2\pi$. Let's think step by step and output the final answer within `\boxed{}`. **[/INST]**

1. **Calculate the radius r :**

$$r = \sqrt{0^2 + 3^2} = \sqrt{0 + 9} = \sqrt{9} = 3.$$

2. **Determine the angle θ :**

- The point $(0, 3)$ is on the positive y -axis.
- The angle θ with the positive x -axis is given by:

$$\theta = \tan^{-1} \left(\frac{3}{0} \right).$$

- Since the point is on the positive y -axis, the angle is $\frac{\pi}{2}$.

3. **Combine the results to get the polar coordinates:**

$$\boxed{(3, \frac{\pi}{2})}$$

Qwen2.5-Math-1.5B

[INST] Cities A and B are 45 miles apart. Alicia lives in A and Beth lives in B . Alicia bikes towards B at 18 miles per hour. Leaving at the same time, Beth bikes toward A at 12 miles per hour. How many miles from City A will they be when they meet? Let's think step by step and output the final answer within `\boxed{}`. **[/INST]**

To determine where Alicia and Beth will meet, we need to find out how long it will take for them to meet and then use that time to calculate the distance Alicia has traveled.

1. First, let's calculate their combined speed. Since Alicia bikes at 18 miles per hour and Beth bikes at 12 miles per hour, their combined speed is $18 + 12 = 30$ miles per hour.
2. Since the distance between the two cities is 45 miles, the time it takes for them to meet is the total distance divided by their combined speed. So, the time t it takes for them to meet is

$$t = \frac{45}{30} = 1.5 \text{ hours.}$$

3. Now, we need to find out how far Alicia has traveled in 1.5 hours. Since Alicia bikes at 18 miles per hour, the distance she travels in 1.5 hours is

$$18 \times 1.5 = 27 \text{ miles.}$$

So, Alicia and Beth will meet 27 miles from City A. The final answer is

27

Table 6: Configuration for Countdown Task

Parameter	Value	Parameter	Value
Pretrained model	Qwen2.5-3B-Instruct	Batch size	128
Generations per prompt	5	Mini-batch size	64
Max prompt length	2,048	Max response length	8,192
Learning rate	1×10^{-6}	Training steps	320
Entropy coefficient	0.001	Clip ratio	0.2
γ_p	0.03	γ_n	0.01
Rollout engine	v11m	Rollout temperature	1
Validation temperature	1	Validation top-k	50
Validation top-p	0.7	Device	2 x A100

C.4 Experimental Details for Section 4.8.2

In this section, we present experimental details to substantiate the claim made in Section 4.8.2: namely, that the Solution Multiplicity Solution Multiplicity(\mathcal{X}), the average number of unique solutions per problem instance, serves as an appropriate metric for evaluating the benefits of encouraging policy entropy in a task. The tasks we consider are as follows:

- **Math Reasoning:** As described in Appendix C.3.
- **Countdown:** As described in Appendix C.1.
- **Countdown-3:** A variant of Countdown where we filter the dataset to retain only samples with three given numbers.
- **Knights and Knaves:** A classic logic puzzle in which the objective is to identify truth-tellers (knights) and liars (knaves) from their statements. (Stojanovski et al., 2025). Below is an example question and correct response.

Knights-and-Knaves

Question:

A very special island is inhabited only by sages and fools. Sages always tell the truth, and fools always lie. You meet 6 inhabitants: Owen, Liam, Evelyn, William, Sofia, and Emily. As Owen put it, "William is a sage". Liam was heard saying, "William is a fool". Evelyn noted, "Sofia is a fool and Evelyn is a sage". "if Owen is a sage then Sofia is a sage." William mentioned. "if Liam is a sage then Evelyn is a sage." Sofia claimed. Emily told you that if Emily is a sage then Liam is a fool. So who is a sage and who is a fool? (Format your answer like: "Owen is a sage/fool, Liam is a sage/fool, Evelyn is a sage/fool, William is a sage/fool, Sofia is a sage/fool, and Emily is a sage/fool") Let's think step by step and output the final answer (should be a sentence) within `\boxed{}`.

Response:

- We need to consider two cases for Owen:
 - *Case 1: Owen is a sage.* If Owen is a sage, then his statement is true. Therefore, William must be a sage.
 - *Case 2: Owen is a fool.* If Owen is a fool, then his statement is false. Therefore, William must be a fool.
- **Liam's statement:** "William is a fool."
 - *Case 1: Liam is a sage.* If Liam is a sage, then his statement is true. Therefore, William must be a fool.
 - *Case 2: Liam is a fool.* If Liam is a fool, then his statement is false. Therefore, William must be a sage.
- **William's statement:** "If Owen is a sage then Sofia is a sage."
 - Since Sofia is a sage, William's statement is true. Therefore, William must be a sage.

- **Owen’s statement revisited:** “William is a sage.”
Since William is a sage, Owen’s statement is true. Therefore, Owen must be a sage.
- **Liam’s statement revisited:** “William is a fool.”
Since William is a sage, Liam’s statement is false. Therefore, Liam must be a fool.
- **Emily’s statement revisited:** “If Emily is a sage then Liam is a fool.”
Since Emily is a sage (from earlier), according to her statement, Liam must be a fool. This confirms our previous determination.
- **Owen’s initial statement:** “William is a sage.”
Since Owen is a sage and William is a sage, Owen’s statement is true. This is consistent.

Therefore, summarizing:

- Owen is a sage.
- Liam is a fool.
- Evelyn’s statement was a contradiction, so Evelyn must be a fool.
- William is a sage.
- Sofia is a sage.
- Emily’s statement was consistent, so Emily must be a sage.

Owen is a sage, Liam is a fool, Evelyn is a fool, William is a sage, Sofia is a sage, and Emily is a sage

To estimate Solution Multiplicity, we query the GPT-5-Think model on 200 randomly selected samples with the following prompt:

Prompt for Querying Solution Multiplicity

[INST]You are an expert mathematics educator and problem solver. Analyze the given mathematical problem and determine how many different solution approaches exist for it.

Please provide a comprehensive analysis that: 1. Identifies all distinct solution methods/approaches
2. Briefly explains what each approach involves 3. Counts the total number of different approaches

Mathematical Problem: problem

Please first explain what different solution approaches exist for this problem, then provide your final answer in the format: <ways> [number] </ways>

For example, if a problem has exactly 2 different solution methods, your response should end with:
<ways> 2 </ways> **[/INST]**

Table 7: Illustration of Experimental Result

Task	Knight and Knaves	Math	Countdown-3	Countdown
Solution Multiplicity	1.5	3.7	6.5	15.7
Pass@8 of GRPO	47.1	78.6	97.7	73.4
Pass@8 of GRPO + Entropy bonus	38.1	72.6	98.7	76.8
Entropy Effect for Pass@8	-9.0%	-6.0%	+1.0%	+3.4%

Training details. The training setups of Math reasoning and Countdown task are identical to the main experiments as described in Appendix C.1 and C.3. For Countdown-3, we train the model for 160 steps. For GRPO with entropy bonus, we use a bonus coefficient of $\eta_+ = 0.05$. Other configurations are identical to those of the main experiment. For Knights-and-Knaves, we RL fine-tune the Qwen2.5-7B-Instruct [Qwen Team \(2024\)](#) model with LoRA adaptation (rank 256) ([Hu et al., 2022](#)) for 100 steps. We use a learning rate of 4×10^{-5} and a batch size of 32, with 8 rollouts per sample.

Result Analysis. The experimental results, presented in Table 7, reveal a direct correlation between Solution Multiplicity and the efficacy of entropy regularization. Specifically, as a task’s Solution Multiplicity increases, so does the performance gain (Pass@8) of an entropy bonus over vanilla GRPO. This provides strong empirical support for our hypothesis: for tasks with a larger solution space, the benefits of enhanced diversity outweigh the potential trade-offs in single-solution correctness. These findings thus validate

Solution Multiplicity as a practical metric for guiding the decision of whether to increase or decrease entropy for a given task.

D Additional Experimental Results for Countdown

In this section, we provide additional results for the Countdown task.

D.1 Additional Experiments for Entropy coefficient

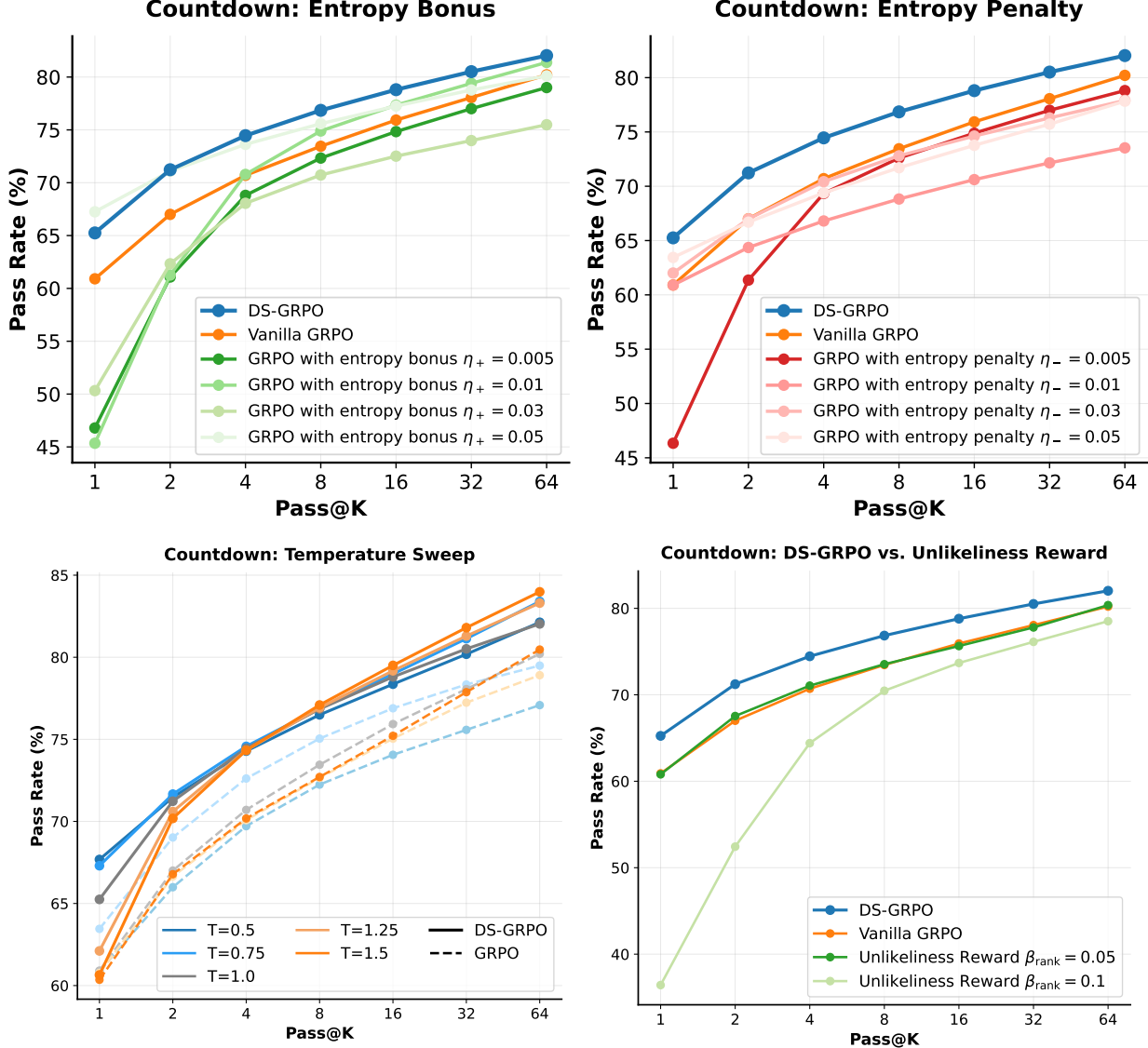


Figure 5: Additional results on the Countdown task comparing DS-GRPO with various baselines. Top: Pass@K performance of DS-GRPO and GRPO under entropy bonus and entropy penalty. Bottom Left: Pass@K performance of DS-GRPO and GRPO across different sampling temperatures. Bottom Right: Pass@K performance of DS-GRPO and the Unlikeliness Reward method with varying coefficients.

To provide a more comprehensive comparison, we analyze the performance of the entropy-based baselines across their full hyperparameter sweep. We compare DS-GRPO against GRPO with varying entropy bonus (η_+) and penalty (η_-) coefficients, with the results illustrated in Figure 5 (Top). The figure clearly

demonstrates that DS-GRPO consistently outperforms the global entropy control methods across their entire range of tested hyperparameters for all values of K .

D.2 Effects of KL Coefficient and Other Factors

Figure 5 (Bottom Left) reports results with varying sampling temperatures for both DS-GRPO and GRPO. Under the same temperature, DS-GRPO achieves consistently higher Pass@ K .

Figure 5 (Bottom Right) presents results from varying the unlikeliness reward coefficient $\beta_{\text{rank}} \in \{0.05, 0.1, 0.15, 0.2, 0.25, 0.3\}$ (He et al., 2025a). For $\beta_{\text{rank}} \geq 0.15$, training collapses and accuracy drops to 0, so we omit those results.

E Additional Experimental Results for Math Reasoning Experiment

E.1 Additional Experimental Results on DS-GRPO vs GRPO

Experimental Results. Figure 6, which contains the full results for Section 4.4, compares our proposed DS-GRPO against the vanilla GRPO baseline across three different base models and five mathematical reasoning benchmarks. The results consistently demonstrate that DS-GRPO outperforms vanilla GRPO across all tested models and datasets.

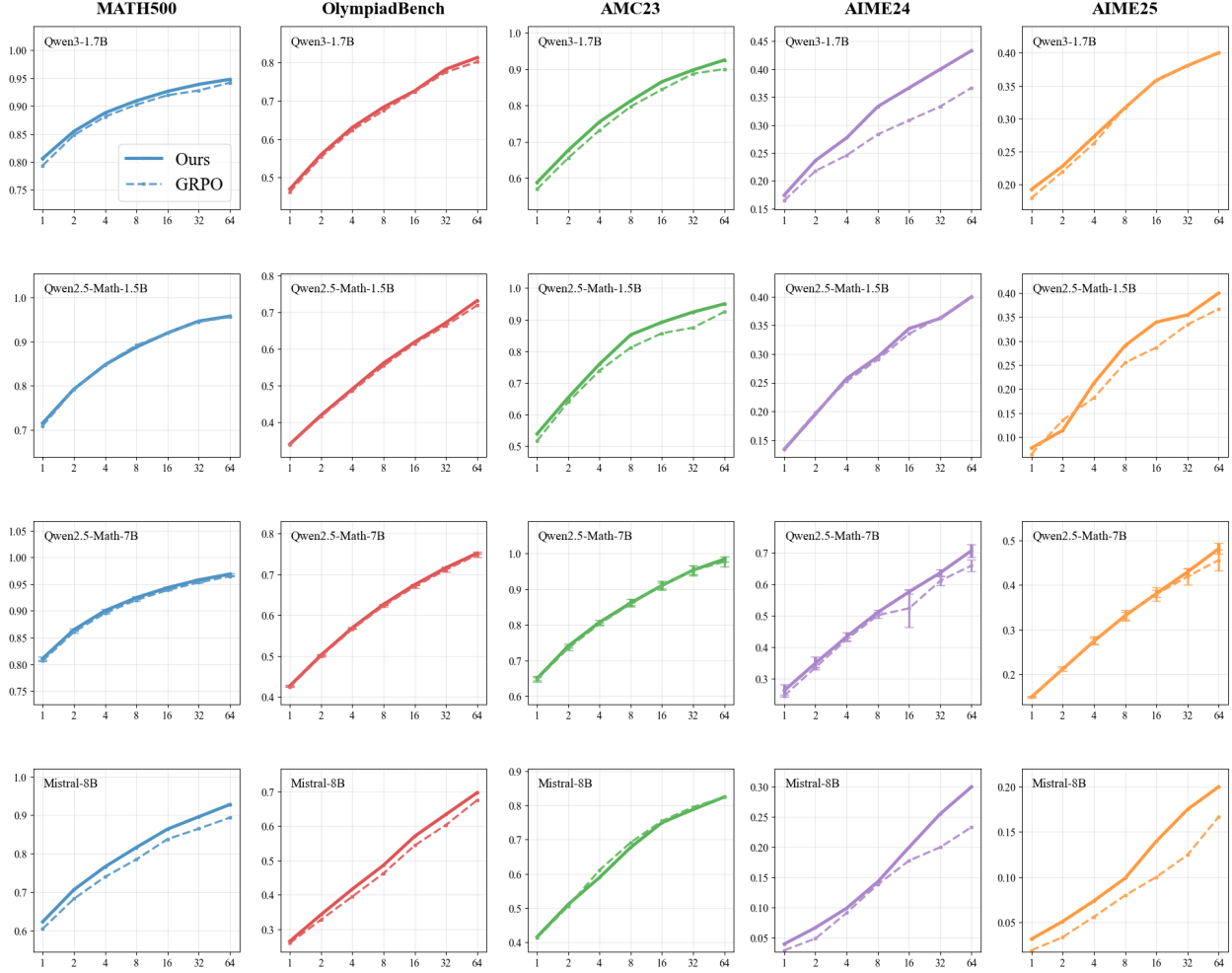


Figure 6: Pass@K performance after reward modification, compared with vanilla GRPO. X-axis denotes K and y-axis denotes pass rates. Trained on the DAPO([Yu et al., 2025](#)) and the MATH([Hendrycks et al., 2021](#)) Dataset.

E.2 Additional Ablation Study for DS-GRPO

Ablation Study Implementation. To isolate the contribution of each component in our reward modification strategy, we conduct an ablation study. We compare the full DS-GRPO algorithm against two specialized variants: *DS-GRPO-Positive*, which only modifies the advantage for correct trajectories, and *DS-GRPO-Negative*, which only modifies the advantage for incorrect trajectories.

Their respective advantage modifications are defined as follows:

$$A_i^{\text{DS}^+} = A_i - \gamma_p \log \pi_{\theta_{\text{old}}}(y_i | x), \quad \text{if } r_i = 1,$$

$$A_i^{\text{DS}^-} = A_i + \gamma_n \log \pi_{\theta_{\text{old}}}(y_i | x), \quad \text{if } r_i \neq 1.$$

The DS-GRPO-Positive variant applies only the modification to correct trajectories ($A_i^{\text{DS}^+}$), leaving the advantage for incorrect trajectories as the standard A_i . Conversely, the DS-GRPO-Negative variant applies only the modification to incorrect trajectories ($A_i^{\text{DS}^-}$), leaving the advantage for correct trajectories unchanged. **Result Analysis.** We present the results of our ablation study in Figure 7. The key findings

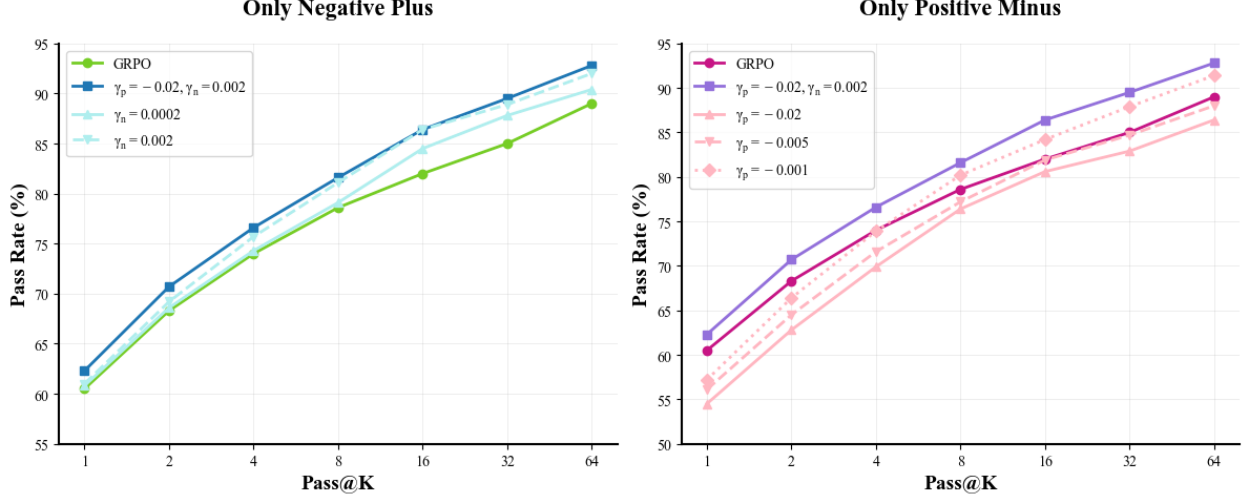


Figure 7: Comparison on Different Hyperparameter of DS-GRPO.

are as follows:

- *DS-GRPO-Positive vs. Vanilla GRPO.* As shown in Figure 7, DS-GRPO-Positive outperforms vanilla GRPO, particularly for larger values of K . This demonstrates that modifying the reward for correct trajectories successfully mitigates the sharpening effect, providing empirical support for our intuition in Section 3.4 that penalizing high-probability correct solutions enhances diversity.
- *DS-GRPO-Negative vs. Vanilla GRPO.* The figure also shows that DS-GRPO-Negative consistently outperforms vanilla GRPO across all values of K . This indicates that modifying the reward for incorrect trajectories is effective at improving the model's overall correctness.
- *DS-GRPO vs. Its Components.* The full DS-GRPO algorithm demonstrates superior performance over both of its individual components (DS-GRPO-Positive and DS-GRPO-Negative) for all K . This highlights a clear synergy: the "Positive" component drives diversity, while the "Negative" component enhances correctness. Their combination in DS-GRPO achieves the best balance, validating our complete reward modification strategy as outlined in Section 3.4.

E.3 Additional Experiment on Comparing DS-GRPO with CISPO

We compare DS-GRPO with CISPO (Chen et al., 2025a), as illustrated in Figure 8. The results demonstrate that DS-GRPO consistently achieves a higher Pass@K compared to CISPO across all datasets. All experiments were conducted using the Qwen2.5-Math-1.5B model.

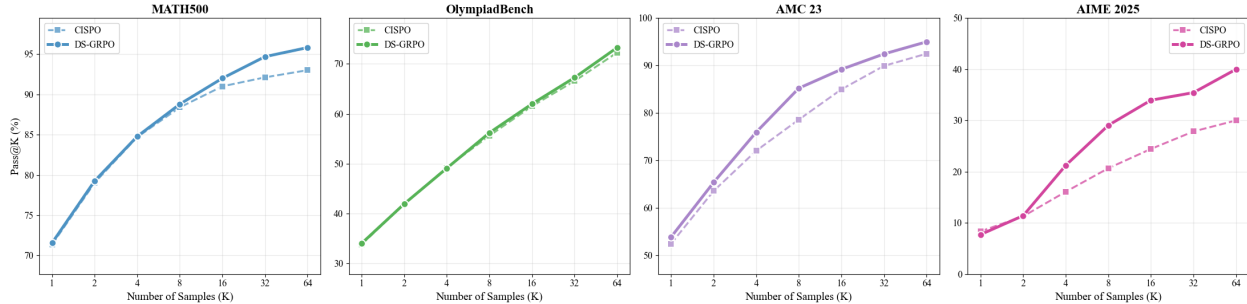


Figure 8: Comparison on CISPO with DS-GRPO.